MASTERARBEIT | MASTER'S THESIS

Titel | Title

Dissecting the Genetic Basis of Brain Asymmetry in Drosophila melanogaster

verfasst von | submitted by

Leonard Alexander Schönsteiner

angestrebter akademischer Grad | in partial fulfilment of the requirements for the degree of

Master of Science (MSc)

Wien | Vienna, 2026

Studienkennzahl lt. Studienblatt | Degree programme code as it appears on the student record sheet:	UA 066 878
Studienrichtung lt. Studienblatt | Degree programme as it appears on the student record sheet:	Masterstudium Cognition, Behavior and Neurobiology
Betreut von | Supervisor:	Univ.-Prof. Dr. Thomas Hummel

Table of Contents

Abstract

Brain asymmetry is a common feature of bilaterian nervous systems and most likely contributes to efficient parallel information processing by hemispheric specialization and behavior. In *Drosophila melanogaster*, the Asymmetrical Body (AB) of the Central Complex offers a powerful model for studying circuit lateralization at cellular resolution, yet the molecular mechanisms establishing dircetional lateralization remain insufficiently understood. In this study, a forward genetic screen using RNAi technique was conducted. Individual genes were knocked down either in single neuronal populations or in combined populations to test whether their loss disrupts AB lateralization. Lateralization phenotypes were then assessed, and genes exceeding a predefined threshold were selected for further analysis. Two candidates, 18-wheeler (18w) and Dpr-interacting protein ζ (DIP ζ), initially produced elevated bilateral phenotypes; however, only DIP ζ showed reproducible effects in the rescreen.

DIP ζ knockdown robustly increased lateralization phenotypes, with the strongest effects observed when both AB afferent (input) and efferent (output) neurons were targeted simultaneously. This suggests that DIP ζ function is required within the interconnected circuit formed by those neurons. Developmental profiling further revealed that bilateral projections are already present at early pupal stages, suggesting that DIP ζ influences the remodeling processes that normally eliminate SA^{uni} axons in the left brain hemisphere. In contrast, knockdown in afferent neurons alone did not produce pupal phenotypes but led to reduced AB circuit lateralization only in adulthood, implying an additional, later role of DIP ζ in maintaining circuit lateralization in a cell-specific manner.

Overall, this work identifies DIP ζ as a previously uncharacterized regulator of AB lateralization in *Drosophila melanogaster*. These findings highlight the importance of cell adhesion molecules in circuit remodeling and they provide a basis for future studies dissecting the molecular logic of hemispheric specialization.

Zusammenfassung

Hirnasymmetrie ist ein häufiges Merkmal bilateraler Nervensysteme und trägt vermutlich zu einer effizienten parallelen Informationsverarbeitung durch hemisphärische Spezialisierung und verhaltensbezogene Differenzierung bei. In *Drosophila melanogaster* bietet der Asymmetrische Körper (Asymmetrical Body, AB) des Zentral Komplexes (Central Complex, CX) ein leistungsfähiges Modellsystem, um lateralisierte neuronale Verschaltungen auf zellulärer Ebene zu untersuchen. Dennoch sind die molekularen Mechanismen, die eine gerichtete Lateralität etablieren, bisher nur unzureichend verstanden. In dieser Studie wurde ein forward-genetischer Screen mittels RNAi durchgeführt. Einzelne Gene wurden entweder in spezifischen neuronalen Populationen oder gleichzeitig in mehreren miteinander verschalteten Zelltypen herunterreguliert, um zu testen, ob deren Verlust die AB-Lateralisation beeinträchtigt. Anschließend wurden Lateralitätsphänotypen quantifiziert und Gene, die einen vordefinierten Schwellenwert überschritten, für weiterführende Analysen ausgewählt. Zwei Kandidaten, 18-wheeler (18w) und Dpr-interacting protein ζ (DIP ζ), zeigten zunächst erhöhte bilaterale Phänotypen; jedoch erwies sich ausschließlich DIP ζ im Rescreen als reproduzierbar.

Die Herunterregulierung von DIP ζ führte konsistent zu verstärkten Lateralitätsdefekten, wobei die deutlichsten Effekte auftraten, wenn sowohl AB-afferente (Input-) als auch AB-efferente (Output-) Neuronen gleichzeitig betroffen waren. Dies deutet darauf hin, dass DIP ζ innerhalb dieses verschalteten neuronalen Kreises benötigt wird. Entwicklungsanalysen zeigten zudem, dass bilaterale Projektionen bereits im frühen Puppenstadium auftreten, was darauf hindeutet, dass DIP ζ jene Remodellierungsprozesse beeinflusst, die normalerweise zum Rückzug der SA^{uni}-Axone aus der linken Gehirnhemisphäre führen. Im Gegensatz dazu verursachte die alleinige Herunterregulierung in den afferenten Neuronen keine pupalen Phänotypen, sondern reduzierte die Lateralität des AB-Kreises erst im Erwachsenenstadium. Dies spricht für eine zusätzliche, spätere Funktion von DIP ζ bei der Aufrechterhaltung der korrekten hemisphärischen Verschaltung in einem zelltypspezifischen Kontext.

Insgesamt identifiziert diese Arbeit DIP ζ als bislang unbekannten Regulator der AB-Lateralisation in *Drosophila melanogaster*. Die Ergebnisse unterstreichen die Bedeutung von Zelladhäsionsmolekülen für neuronales Remodeling und liefern eine Grundlage für zukünftige Studien, die die molekulare Logik hemisphärischer Spezialisierung entschlüsseln sollen.

1. Introduction

1.1 Brain asymmetry and its evolutionary significance

Bilateral symmetry is a characteristic feature of the body plan of Bilaterians. It ensures a mirror-image arrangement of the left and right halves of the body, which facilitates movement, orientation, and balanced sensory perception. However, despite this external symmetry, especially the nervous system displays internal left (L)-right (R) differences in structure and function (Corballis, 2021; Güntürkün et al., 2020). Early neuroanatomical studies by Paul Broca in 1861 demonstrated the dominance of the Left brain hemisphere (LHS) for language processing in humans and showed that damage to the Left frontal convolution impaired articulate speech (Broca, 1861; Graham, 2022). These observations highlighted early on that the human central nervous system (CNS) is not simply symmetrical, but rather that different regions in the left and right hemispheres exhibit different connectivity, anatomy, and cognitive functions (Toga et al., 2009).

This functional and structural lateralization of the CNS appears to be a shared characteristic rather than a random by-product of development. Comparative evidence from mammals, birds and invertebrates indicates that lateralized brain organization has deep evolutionary roots. In mammals, for example, hemispheric specialization extends beyond language to include motor control, attention and emotional processing (Güntürkün et al., 2020). In birds, cerebral asymmetries underpin eye preferences and song-learning circuits, showing that L-R brain differences contribute to efficient processing in non-mammalian taxa (Güntürkün et al., 2020). In fishes, amphibians and reptiles, structural asymmetries (such as the habenular complex) as well as population-level lateralized behaviours (e.g., preferential turning, side-biased predator detection) have been documented (Bisazza et al., 1998). Importantly, asymmetry is not limited to humans or even mammals. Behavioural and anatomical lateralization has been shown in invertebrates, for instance, in honey bees (*Apis mellifera*), the olfactory memory recall is stronger when using the right antenna soon after learning, whereas after several hours the left antenna becomes dominant, indicating a functional shift in hemispheric engagement during memory consolidation (Anfora et al., 2010). Together, these insights suggest that lateralization is a common principle of brain organization and provides adaptive advantages.

One proposed functional advantage of brain lateralization is that by segregating competing processes into opposite hemispheres, the brain can reduce duplicate neural "hardware" and minimize redundant processing, thereby increasing cognitive efficiency (Rogers, 1995; Rogers et al., 2013). For instance, human brain asymmetries allow one hemisphere to specialize in language while the other may support spatial or emotional processing, thus promoting parallel information processing. Indeed, meta-analyses link altered cerebral lateralization with neurodevelopmental disorders: patients with autism spectrum disorder (ASD) or schizophrenia often exhibit reduced left-hemisphere dominance for language and other lateralized functions (Floris et al., 2021; Sha et al., 2021). In autism, functional connectivity studies show less left-lateralized language networks compared to neurotypical controls, suggesting that reduced lateralization may reflect compromised specialization rather than simple anatomical variation (Nielsen et al., 2014). In schizophrenia, diminished language lateralization has been documented even at first episode, supporting the hypothesis that disturbed lateral neural networks contribute to pathophysiology (Bleich-Cohen et al., 2009).

1.2 *Drosophila melanogaster* as a model organism for studying brain asymmetry

The vinegar fly *Drosophila melanogaster* (*D. melanogaster*) has long stood as a cornerstone of neurogenetic and developmental research. Despite its small brain size, the brain of *D. melanogaster* is highly organized and allows the animal to perform a variety of complex behaviours including learning, memory formation and navigation, thereby offering a tractable system in which to explore mechanisms underlying higher-order neural functions (Davis, 2005).

One of the most striking recent advances in fly neuroscience is the generation of a fully annotated connectome of the adult fly brain. The international FlyWire Consortium mapped approximately 140 000 neurons and over 50 million synapses, producing the largest and most comprehensive wiring diagram of a brain to date (NIH, 2024; Sanders, 2024). This connectome not only reveals the full "projectome" of different neural circuits (Schlegel et al., 2024) but also provides access to the architecture and inter-hemispheric connectivity of the fly brain.

In addition, *D. melanogaster* offers a powerful genetic toolkit, including binary expression systems such as the GAL4/UAS and LexA/LexAop, which enable precise spatial and temporal targeting of defined neuronal populations (Duffy, 2002; Jenett et al., 2012). Together, these tools offer an efficient platform to dissect how asymmetry is established during development in a highly organized brain of a multicellular organism.

1.3 The Central Complex (CX) lateralization as a model for structural lateralization

The insect Central Complex (CX) is a conserved set of neuropils that forms the core hub for higher-order sensory integration and motor control in *D. melanogaster* (Heinze & Homberg, 2008) (**Figure 1A-E**). The CX has been shown to be especially required for spatial orientation, navigation and decision-making behaviours across insect species (Strausfeld, 2012; Pfeiffer & Homberg, 2014). Structurally, the CX is composed of five interconnected neuropils: the Fan-shaped Body (FB), Ellipsoid Body (EB), Noduli (NO), Protocerebral Bridge (PB) and Asymmetrical Body (AB). Aport from the AB, all CX neuropils exhibit L-R symmetry (Hanesch et al., 1989; Wolff & Rubin, 2018).

The AB is a paired neuropil ventrally embedded into the FB and exhibits consistent L-R differences in size, with the right AB (R-AB) being around 4-fold larger in size than its left counterpart (Pfeiffer & Homberg, 2014; Pascual et al., 2004). In the majority of wild-type flies, the right AB (R-AB) is significantly larger and more densely innervated than its left counterpart (L-AB). This consistent anatomical bias mirrors the hemispheric dominance observed in vertebrate brains and thus provides a tractable system for exploring how lateralized circuits emerge during development (Kaiser, 2017; Riebli et al., 2013).

The AB circuit comprises different afferent and efferent neuron populations that can be genetically labeled and manipulated. SA^{uni} neurons (**Figure 1G**) constitute the principal afferent class and define AB size differences by recruiting their postsynaptic partners specifically to the R-AB. They innervate the AB unilaterally and therefore provide the key asymmetry-driving input to this circuit. SA^{bi} neurons (**Figure 1F**) represent the main afferent population innervating the L-AB and, in contrast to SA^{uni} neurons, they project bilaterally to both hemispheres. vΔ neurons (**Figure 1H**) serve a the major efferent output neurons of the AB

circuit. They form synapses with both SA neuron classes in the R-AB, but in the L-AB they synapse exclusively with SA^{bi} neurons, while maintaining a bilateral overall projection pattern (Pascual et al., 2004; Riebli et al., 2013; Kaiser, 2017; Lapraz et al., 2023).

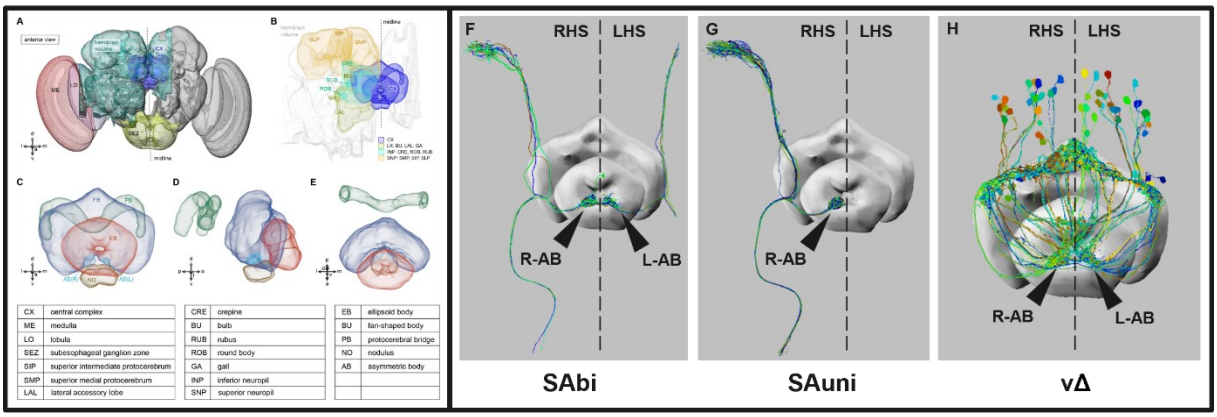

Figure 1. Anatomy of the *Drosophila melanogaster* Central Complex (CX) and projection patterns of AB-associated neuron populations:
A frontal view of the *Drosophila melanogaster* brain (**A**) illustrates the overall brain anatomy. The Central Complex (CX) is highlighted in dark blue, and the anatomical midline is indicated by a dashed black line. Major brain regions that are largely located outside the hemibrain volume, including the lobula (LO), medulla (ME), and subesophageal zone (SEZ), are labeled for orientation. A closer view of the hemibrain region (**B**) shows the CX together with adjacent accessory neuropils. Detailed views of the individual CX substructures are shown in a frontal orientation (**C**), as well as in lateral (**D**) and dorsal (**E**) orientations, including the ellipsoid body (EB), fan-shaped body (FB), protocerebral bridge (PB), paired noduli (NO), and Asymmetrical Body (AB). Panels **A-E** are adapted from Hulse et al. (2021).
The projection patterns of AB-associated neuron populations are shown in panels **F-H**. SA^{bi} afferent neurons (**F**) innervate the Asymmetrical Body bilaterally, projecting to both the right and left brain hemispheres, as indicated by arrows. In contrast, SA^{uni} afferent neurons (**G**) display a unilateral projection pattern restricted to the right hemisphere, with the arrow marking the right Asymmetrical Body (R-AB). vΔ neurons (**H**) represent the principal efferent population of the AB and extend projections across both hemispheres. In panels **F-H**, the dashed black line marks the anatomical midline separating the right hemisphere (RHS) from the left hemisphere (LHS). Neuron visualizations were generated using the hemibrain neuron visualization platform https://hemibrain.neuronlp.fruitflybrain.org/.
Abbreviations: AB = Asymmetrical Body; CX = Central Complex; EB = ellipsoid body; FB = fan-shaped body; PB = protocerebral bridge; NO = nodulus; LO = lobula; ME = medulla; SEZ = subesophageal zone; RHS = right hemisphere; LHS = left hemisphere; R-AB = right Asymmetrical Body; L-AB = left Asymmetrical Body.

Over the past years, different molecular players involved in the development of AB asymmetry have been identified. For instance, the guidance cue Netrin B (NetB) and its receptor Frazzled (Fra) have been shown to direct SA^{uni} axons preferentially toward the right hemisphere during AB circuit formation (Lapraz et al., 2023). Manipulating these molecules disrupts the normally right-biased innervation pattern of SA^{uni} neurons, leading to bilateral or inverted AB innervation, resulting in alterations in overall AB neuropil asymmetry. Furthermore, the cell-adhesion molecule Fasciclin II (FasII), the *D. melanogaster* homolog of the vertebrate neural

cell adhesion molecule (NCAM) (Hortsch, 1996), has been implicated in the early lateralization of the AB circuit.

In wild-type development, SA^{uni} neurons initially exhibit a bilateral projection pattern, representing the developmental ground state of the AB circuit (Pascual et al., 2004; Lapraz et al., 2023). During metamorphosis, these transient left-side branches are selectively removed, resulting in the characteristic unilateral innervation of the R-AB. This transition from bilateral to unilateral connectivity provides the basis for the emerging asymmetry of the AB neuropil (**Figure 2**).

Recent findings demonstrated that FasII is crucial for the retraction of SA^{uni} neurons during brain development in a cell non-autonomous fashion (Markovitsch et al., 2025). When FasII expression is selectively reduced in SA^{bi} neurons, the number of bilateral phenotypes significantly increases (Markovitsch et al., 2025), suggesting that SA^{bi} neurons support axonal retraction of SA^{uni} neurons from the L-AB.

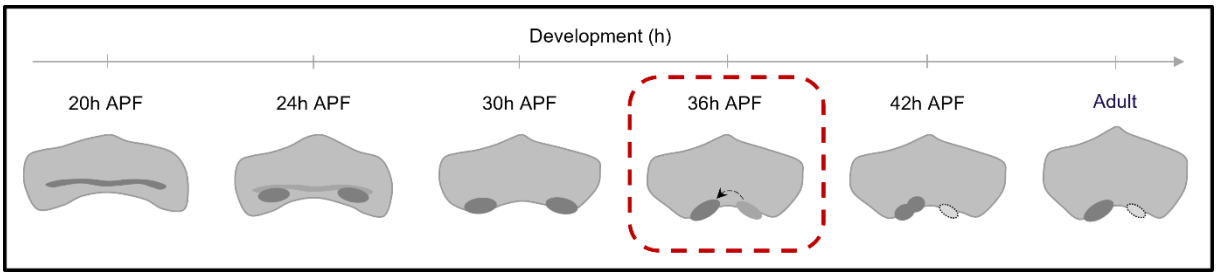

Figure 2. Progressive remodeling of SA^{uni} projections during pupal development:
The figure illustrates the stepwise remodeling of SA^{uni} neuron projections during pupal development, focusing on their innervation of the Asymmetrical Body (AB). Representative developmental stages are arranged from left to right, with a horizontal arrow indicating the temporal progression from early pupal stages to adulthood. At 20h after puparium formation (APF), the basic structure of the AB is present and SA^{uni} neurons project bilaterally. At 24h APF, pruning of left-sided SA^{uni} branches is initiated, followed by a progressive reduction of left projections at 30h APF. By 36h APF, active pruning is evident and a pronounced right-sided bias begins to emerge; this stage is highlighted to indicate a critical phase of circuit remodeling. At 42h APF, left-side retraction is completed and right-sided projections are stabilized. In the adult brain, SA^{uni} neurons display a fully established unilateral innervation of the right Asymmetrical Body (R-AB). Together, the schematics depict the transition from an initially symmetric projection pattern to a stable, right-lateralized circuit architecture.
This schematic representation is based on developmental data reported in Markovitsch et al. (2025).
Abbreviations: APF = after puparium formation; h = hours; AB = Asymmetrical Body; R-AB = right Asymmetrical Body.

1.4 Aims and rationale of this study

Although some key molecular and cellular players contributing to the establishment of CX asymmetry in *D. melanogaster* have been identified, the molecular mechanisms that translate

early cellular interactions into stable, lateralized connectivity remain largely unresolved. In particular, it is still unclear how specific neuron classes, such as SA^{uni}, SA^{bi}, and vΔ, interact through molecular cues like Fasciclin II (FasII) and Netrin B (NetB) to achieve and maintain the right-sided dominance of the Asymmetrical Body (AB). Previous studies have shown that loss of FasII or disruptions in Netrin signaling can interfere with proper AB wiring and lead to bilateral phenotypes (Mitic, 2021; Markovitsch et al., 2025). However, many of the genes and pathways known to influence neural patterning in other parts of the brain have not yet been systematically tested in the AB circuit, leaving major knowledge gaps in the genetic architecture underlying its lateralization.

The aim of this study is therefore to identify novel genes required for the correct development of AB lateralization in the *D. melanogaster* brain. To address this, an RNA interference (RNAi)-based forward genetic screen was performed to systematically knockdown candidate genes potentially involved in AB asymmetry within defined afferent and efferent AB neuron populations.

In an initial screen, 20 fly lines (**Table 1**) carrying transgenic UAS-RNAi constructs were crossed with a GAL4 driver line (*;R72A10-LexA,LexAop-mCD8::GFP,per-GAL4/CyO;R70H05-GAL4/TM2*) that targets both SA^{uni} afferent neurons and vΔ efferent neurons of the AB circuit (**Table 2**). This approach allowed targeted post-transcriptional gene silencing within the AB network in the F1 generation. These were analyzed for lateralization phenotypes using confocal microscopy. Brains showing disrupted AB lateralization were categorized and quantified to assess gene-specific effects on central brain asymmetry.

To verify and refine the results, a secondary screen (rescreen) was conducted under the same conditions. This rescreen focused on candidate genes that exhibited elevated rates of bilateral phenotypes in the initial screen. In addition to the original GAL4 driver targeting afferent and efferents together, several neuron-type-specific GAL4 lines were employed (**Table 2**) to determine in which neuronal populations the identified genes are required.

Finally, to gain insight into the temporal requirement of the identified candidates, pupal dissections were performed. By comparing pupal and adult brains, the aim was to determine whether the identified molecule is required during the initial remodeling phase of AB formation or is instead required later to maintain asymmetry into adulthood.

Together, this stepwise screening strategy aimed to uncover novel molecular regulators underlying the establishment and maintenance of brain asymmetry in *D. melanogaster*.

2. Materials and Methods

2.1 Materials

2.1.1 Fly Lines

Table 1. Overview of RNAi transgenic lines and their source repositories:
Gene names are reported as listed by the respective stock centers. VDRC = Vienna Drosophila Resource Center. NIG = National Institute of Genetics. Identification number in brackets.

Gene	Source
midline fasciclin	VDRC (37888)
Neurexin 1	VDRC (36328)
Cadherin 86C	VDRC (21327)
Dpr-interacting protein ζ	VDRC (38261)
Cad99C	VDRC (27212)
Immunoglobulin domain subtype	VDRC (43603)
18 wheeler	VDRC (44386)
CLASS B SCAVENGER RECEPTORS	VDRC (10272)
center divider, NON-RECEPTOR TKL KINASES	VDRC (43634)
Pitslre	VDRC (45127)
Rab18	VDRC (40228)
Annexin B11	NIG (9093R-3)
Tetraspanin 39D	VDRC (37127)
Golgi complex-localized glycoprotein 1	VDRC (31070) (CG7190)
Mucin 12Ea	VDRC (50435)
Eps15 homology domain containing protein-binding protein 1	VDRC (43406)
vanin-like	VDRC (50592)
Leucine-rich repeat protein	VDRC (44988)
croquemort	VDRC (45884)
uninflatable	VDRC (1047) (CG9138)

Table 2. Overview of GAL4 driver lines:
Full genotypes and source information are reported according to the original suppliers.

Driver	Genetics	Source
elav C155-GAL4 ;repo-GAL4	*elav^{C155}-GAL4/FM7a;;repo-GAL4/TM3*	Bloomington Drosophila Stock Center #458 (*elav*) Bloomington Drosophila Stock Center #7415 (*repo*)
R70H05-GAL4 (vΔ)	*;R72A10-LexA,LexAop-mCD8::GFP/CyO;R70H05-GAL4/TM2*	Bloomington Drosophila Stock Center #39554 (*R70H05*) Bloomington Drosophila Stock Center #54191 (*R72A10*)
per-GAL4 (SA^{uni})	*;per-GAL4, R72A10-LexA,LexAop-mCD8::GFP/CyO;TM2/TM3*	Bloomington Drosophila Stock Center #7127
fas2^{Mz507}-GAL4 (SA^{bi})	*fas2^{Mz507}-GAL4; R72A10-LexA,LexAop-mCD8::GFP/CyO;*	Sulzbacher et al., 1997
R70H05-GAL4 (vΔ); per-GAL4 (SA^{uni})	*;R72A10-LexA,LexAop-mCD8::GFP,per-GAL4/CyO;R70H05-GAL4/TM2*	Bloomington Drosophila Stock Center #39554 (*R70H05*) Bloomington Drosophila Stock Center #7127 (*per-GAL4*) Bloomington Drosophila Stock Center #54191 (*R72A10*)
empty-GAL4	*;R72A10-LexA,LexAop-mCD8::GFP/CyO;empty-GAL4/TM6*	Hummel Lab, University of Vienna

2.1.2 Antibodies

Table 3. Overview of antibodies applied for immunohistochemical staining:
Includes primary and secondary antibodies with host species and supplier information. DSHB = Developmental Studies Hybridoma Bank

Type	Antibody	Origin	Source
Primary	α-NCadherin (Ncad)	Rat	DSHB
Primary	α-Fasciclin II (FasII)	Mouse	DSHB
Secondary	α-Rat Alexa 647	Goat	Invitrogen
Secondary	α-Mouse Alexa 568	Goat	Invitrogen
Secondary	α-Mouse Alexa 488	Goat	Invitrogen
Secondary	α-Mouse Alexa 488	Goat	Invitrogen

2.2 Methods

2.2.1 Fly stocks

D. melanogaster stocks were kept on standard cornmeal-agar medium and maintained in climate-controlled incubators at 25°C. When stronger GAL4-dependent expression was required, for example to increase the efficiency of RNAi constructs, experimental crosses were additionally reared at 29°C, a temperature known to enhance GAL4/UAS transcriptional output (Brand & Perrimon, 1993).

To generate progeny for the 29°C condition, adult flies were placed at 25°C for several days to allow egg deposition. After 2-3 days, the parental flies were removed and the vials containing embryos or early larvae were shifted to 29°C, where they remained for the rest of development.

Adult brains were dissected from flies aged 3-5 days post-eclosion. For pupal analyses, individuals were collected at the white-prepupa stage (0 h after puparium formation, APF), transferred to fresh vials, and allowed to develop until the desired time point (50h APF) before dissection.

2.2.2 Binary expression system

To obtain precise spatial and temporal control of gene expression, this work uses well-established binary transcriptional systems such as GAL4/UAS (Brand & Perrimon, 1993) and LexA/LexAop. These systems enable expression of effectors (for example, fluorescent reporters or RNAi constructs) exclusively in specified cell populations.

In the GAL4/UAS system, a driver line expresses the yeast transcription factor GAL4 under a cell-type or tissue-specific promoter, which then binds to UAS (Upstream Activating Sequence) sites located upstream of the effector gene. The LexA/LexAop system operates analogously, with LexA as the driver factor and LexAop as the regulatable upstream activation element. Using two such systems either separately or in combination allows for fine control and/or intersectional expression of transgenes (Ting et al., 2011).

In this project, RNAi-mediated gene silencing was achieved through the GAL4/UAS system, while neuronal populations of interest were visualized by expressing GFP via the LexA/LexAop system, allowing both approaches to be combined within the same specimen.

2.2.3 RNA interference approach

RNA interference (RNAi) provides a method to reduce gene expression at the mRNA level, enabling functional analysis without modifying genomic DNA. When combined with binary transcription systems such as GAL4/UAS, this approach makes it possible to suppress specific genes only within genetically defined neuronal populations. In cells where GAL4 is active, a UAS-RNAi construct produces double-stranded RNA, which is subsequently cleaved by Dicer

into small interfering RNAs (siRNAs). These siRNAs guide the RNA-induced silencing complex (RISC) to complementary mRNA molecules, resulting in their degradation and a decrease in the corresponding protein product (Dietzl et al., 2007).

2.2.4 Immunohistochemistry

Adult and pupal *D. melanogaster* brains were carefully dissected in phosphate-buffered saline (PBS) under a stereomicroscope to maintain tissue integrity. Immediately after dissection, samples were fixed in 4% paraformaldehyde (PFA) prepared in PBS for 20 minutes at room temperature, ensuring preservation of neural structures and antigenicity (Wu & Luo, 2006).

Following fixation, the PFA solution was removed, and the brains were washed four times for 20 minutes each in 0.3% PBT (PBS containing 0.3% Triton X-100) to eliminate residual fixative and enhance tissue permeability. Subsequently, samples were incubated in 10% normal goat serum (NGS) diluted in PBT for approximately 1 hour at room temperature to block nonspecific antibody binding (Couto et al., 2005).

Primary antibodies (**Table 3**) were then applied, and the tissue was incubated overnight at 4°C to allow specific antigen-antibody interactions. On the following day, brains were washed thoroughly in PBT and incubated again overnight at 4°C with the corresponding fluorophore-conjugated secondary antibodies (**Table 3**).

After a final series of washes in PBT (4 × 20 minutes), samples were mounted in VECTASHIELD® mounting medium (Vector Laboratories) to preserve fluorescence and prevent photobleaching. A small layer of modeling clay was used as a spacer between the microscope slide and coverslip to avoid tissue compression and maintain the three-dimensional structure of the brain during imaging (Jefferis et al., 2007).

2.2.5 Confocal imaging and data acquisition

Adult and pupal brains were imaged using a Leica TCS SP5 II confocal microscope equipped with a 20× oil immersion objective. Confocal stacks were acquired at a resolution of 512 × 512 pixels, with a scanning speed of 400 Hz and an optical section thickness of approximately 1.5

µm. For each sample, z-stacks covering the entire central brain were obtained to allow full visualization of the Asymmetrical Body (AB) region and its associated neuron types.

Image data were processed and analyzed using Fiji (ImageJ®, NIH, USA) for visualization, reconstruction and quantification of innervation patterns. GFP and FasII signals were examined to classify each brain as unilateral (wild-type-like) or bilateral (phenotypic), following established procedures (Pascual et al., 2004; Scheffer et al., 2020).

Phenotypic data were compiled in Microsoft Excel and R (R Foundation for Statistical Computing, www.r-project.org) for statistical evaluation. Differences in bilateral phenotype frequencies between RNAi knockdown lines and the control (*empty-GAL4*) were tested using Chi-square (χ^2) tests. To minimize false-positive results arising from multiple comparisons, Bonferroni correction was applied to adjust the significance threshold accordingly (Sha et al., 2021).

3. Results

3.1 Initial RNAi screen

First, an initial RNAi screen was performed targeting 20 genes, each tested using the *per-GAL4/AB4-GAL4* driver line, which labels both afferent (SA^{uni} and SA^{bi}) and efferent (vΔ) neurons of the AB circuit (**Figures 3 & 4**). This driver combination allowed cell-type-specific gene knockdown to assess whether AB asymmetry was affected. A loss of asymmetry was defined by the occurrence of bilateral AB innervation of SA^{uni} neurons (**Figure 5**). For simplification, the *per-GAL4/AB4-GAL4* driver is referred to as *SA^{uni}-GAL4/vΔ-GAL4* from here on.

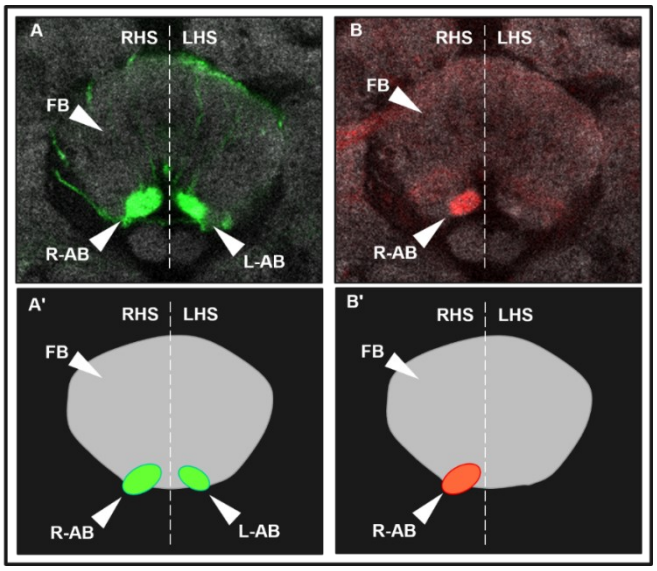

Figure 3. Projection pattern of vΔ neurons into the Asymmetrical Body:
Confocal images illustrate the projection pattern of vΔ neurons within the central brain. In panel **A**, vΔ neurons labeled with green fluorescent protein (GFP) innervate both the right and left Asymmetrical Body (R-AB and L-AB), demonstrating a bilateral projection pattern. A corresponding simplified schematic representation of vΔ neuron projections is shown in panel **A'**. In panel **B**, SA^{uni} neuron innervation is visualized using the synaptic marker Fasciclin II (FasII), highlighting the unilateral organization of SA^{uni}-derived connections within the Asymmetrical Body. A simplified schematic of the FasII-stained SA^{uni} projection pattern is shown in panel **B'**. In all panels, arrows indicate the positions of the fan-shaped body (FB), the right Asymmetrical Body (R-AB), and the left Asymmetrical Body (L-AB). The dashed vertical line marks the anatomical midline separating the right hemisphere (RHS) from the left hemisphere (LHS).
Abbreviations: AB = Asymmetrical Body; R-AB = right Asymmetrical Body; L-AB = left Asymmetrical Body; FB = fan-shaped body; RHS = right hemisphere; LHS = left hemisphere; GFP = green fluorescent protein; FasII = Fasciclin II.

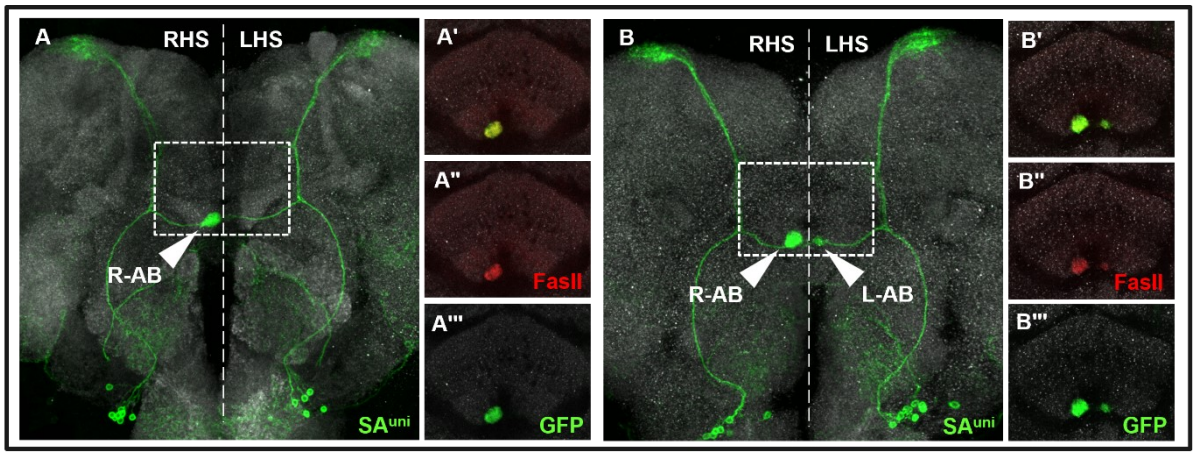

Figure 4. Projection patterns of unilateral and bilateral SA^{uni} neurons into the Asymmetrical Body:
Confocal images illustrate distinct projection patterns of SA^{uni} neurons and their corresponding synaptic organization within the Asymmetrical Body (AB). In panels **A-A''**, wild-type SA^{uni} neurons labeled with green fluorescent protein (GFP) innervate exclusively the right Asymmetrical Body (R-AB), resulting in an unilateral R-AB Fasciclin II (FasII) expression pattern. In panels **B-B''**, an example of bilateral SA^{uni} neuron innervation is shown, in which projections extend to both the right and left Asymmetrical Body (R-AB and L-AB), resulting in a bilateral FasII expression pattern. Panels **A'-A'''** show close-up views of the unilateral R-AB innervation, whereas panels **B'-B'''** show close-up views of the bilateral projection pattern. Overlays of GFP and FasII staining are shown in panels **A' and B'**. Panels **A''-B'''** display individual channels, with FasII staining shown in red to indicate synaptic connections and GFP shown in green to highlight neuronal projections. In all panels, arrows mark the positions of the right and left Asymmetrical Body, and the dashed vertical line indicates the anatomical midline separating the right hemisphere (RHS) from the left hemisphere (LHS).

Abbreviations: AB = Asymmetrical Body; R-AB = right Asymmetrical Body; L-AB = left Asymmetrical Body; RHS = right hemisphere; LHS = left hemisphere; GFP = green fluorescent protein; FasII = Fasciclin II.

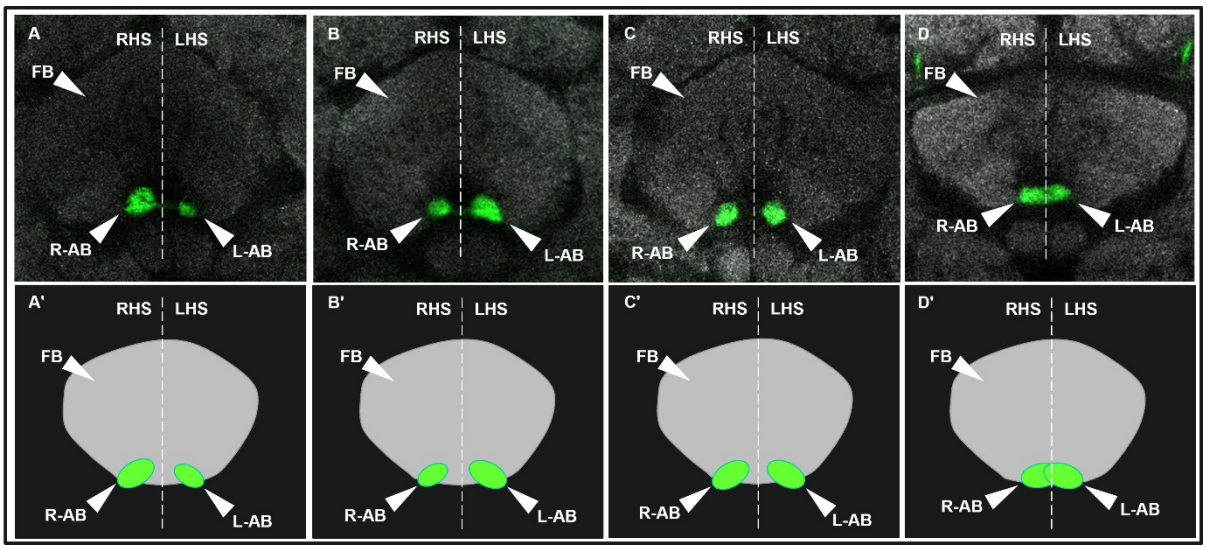

Figure 5. Overview of bilateral projection phenotypes observed in SA^{uni} neurons:
Representative confocal images illustrate distinct classes of bilateral SA^{uni} projection phenotypes into the Asymmetrical Body (AB), together with corresponding schematic representations. Panels **A and A'** show the most common bilateral phenotype, in which both asymmetrical bodies are innervated but the right Asymmetrical Body (R-AB) is larger than the left Asymmetrical Body (L-AB). Panels **B and B'** depict a directionality-disrupted bilateral phenotype, characterized by a larger L-AB compared to the R-AB. In panels **C and C'**, a symmetric phenotype is shown, in which the left and right Asymmetrical Body are approximately equal in size. Panels **D and D'** illustrate a midline-merged phenotype, in which AB projections extend across the midline, resulting in a fused structure; this phenotype was predominantly observed under elevated developmental temperature (29°C). The upper row (**A-D**) shows experimental examples of SA^{uni} projections, whereas the lower row (**A'-D'**) provides simplified schematics summarizing the corresponding projection patterns. In all panels, arrows indicate the positions of the fan-shaped body (FB), the right Asymmetrical Body (R-AB), and the left Asymmetrical Body (L-AB), and the dashed vertical line marks the anatomical midline separating the right hemisphere (RHS) from the left hemisphere (LHS). Abbreviations: AB = Asymmetrical Body; R-AB = right Asymmetrical Body; L-AB = left Asymmetrical Body; FB = fan-shaped body; RHS = right hemisphere; LHS = left hemisphere.

The 20 genes were grouped by molecular function, and each bar in **Figure 6** represents a candidate gene (x-axis) with its corresponding percentage of bilateral phenotypes (y-axis). Bilateral phenotypes included all cases in which SA^{uni} neurons innervated both ABs, ranging from unequal bilateral projections to complete midline fusion of the two ABs (**Figure 5**). Brains were classified as wild-type-like when they exhibited strictly unilateral right-sided innervation.

A threshold of 20% bilateral phenotypes was set as the criterion for selecting candidate genes, ensuring that only knockdowns producing deviations well above the natural baseline variability of AB lateralization, were considered sufficiently strong to warrant further analysis (Mitic et al., 2025, manuscript in prep.). Eight of the twenty RNAi lines showed no lateralization phenotypes (0% bilateral phenotypes), ten lines displayed rates below 20%, consistent with natural variability, and two genes clearly exceeded the threshold (**Table 4**). 18-wheeler (18w)

with 50 lateralization phenotypes (n = 26) and Dpr-interacting protein ζ (DIP ζ) with 31.8% lateralization phenotypes (n = 22).

Both genes were therefore rescreened with the same GAL4 driver line to assess the reproducibility of the initial findings. In parallel, controls were performed using the empty-GAL4 driver to ensure that any observed effects were specifically due to RNAi-mediated knockdown rather than background-related influences.

For 18w, the strong effect on AB lateralization was not reproduced in the rescreen, with the phenotype rate dropping sharply to 3.4% (n = 29), suggesting that the initial observation may have been due to experimental variability. In contrast, DIP ζ knockdown consistently produced a significant increase in bilateral phenotypes (27.3%, n = 33) suggesting a robust role for this gene in AB circuit asymmetry.

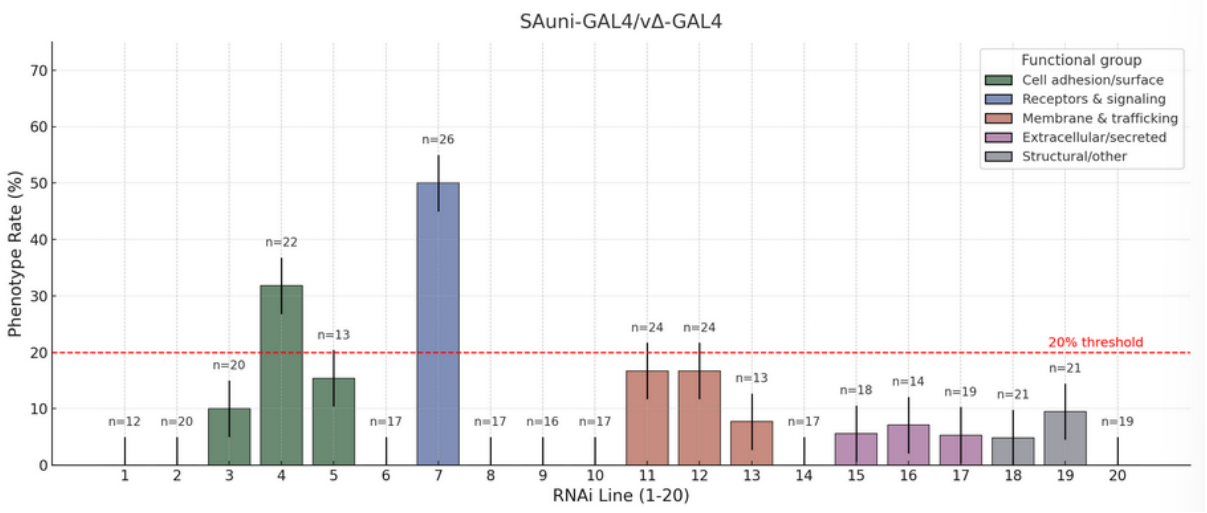

Nr.	Gene	Nr.	Gene
1	*midline fasciclin*	11	*Rab18*
2	*Neurexin 1*	12	*Annexin B11*
3	*Cadherin 86C*	13	*Tetraspanin 39D*
4	*Dpr-interacting protein ζ*	14	*Golgi complex-localized glycoprotein 1*
5	*Cad99C*	15	*Mucin 12Ea*
6	*Immunoglobulin domain subtype*	16	*Eps15 homology domain containing protein-binding protein 1*
7	*18 wheeler*	17	*vanin-like*
8	*CLASS B SCAVENGER RECEPTORS*	18	*Leucine-rich repeat protein*
9	*center divider, NON-RECEPTOR TKL KINASES*	19	*croquemort*
10	*Pitslre*	20	*uninflatable*

Figure 6. Phenotype rates of 20 RNAi candidate genes in the initial *SA^{uni}-GAL4/vΔ-GAL4* screen at 25°C:
The bar graph summarizes the percentage of bilateral phenotypes observed for 20 RNAi-mediated gene knockdowns using the combined *SA^{uni}-GAL4/vΔ-GAL4* driver at 25°C. Each bar represents one candidate gene, plotted along the x-axis according to its RNAi line number, with the corresponding phenotype rate shown on the

y-axis. Error bars indicate variability between analyzed samples, and the number of analyzed brains (n) is indicated above each bar. The red dashed horizontal line marks the predefined threshold of 20% bilateral phenotypes that was used to identify candidates for further analysis. Candidate genes are color-coded according to their functional categories, including cell adhesion or cell-surface proteins (RNAi lines 1-6), receptors and signaling molecules (lines 7-10), membrane-associated and trafficking-related proteins (lines 11-14), extracellular or secreted proteins (lines 15-17), and structural or other proteins (lines 18-20). The table below the graph lists the corresponding gene names for each RNAi line number.
Abbreviations: n = number of analyzed brains; RNAi = RNA interference; GAL4 = galactose-responsive transcription factor GAL4.

Table 4. Results of initial screen for all 20 candidate genes:
N = number of total brains scanned per RNAi line.

RNAi line	N	N (bilaterals)	% (bilaterals)
midline fasciclin	12	0	0.0
Neurexin 1	20	0	0.0
Cadherin 86C	20	2	10.0
Dpr-interacting protein ζ	22	7	31.8
Cad99C	13	2	15.4
Immunoglobulin domain subtype	17	0	0.0
18 wheeler	26	13	50.0
CLASS B SCAVENGER RECEPTORS	17	0	0.0
center divider, NON-RECEPTOR TKL KINASES	16	0	0.0
Pitslre	17	0	0.0
Rab18	24	4	16.7
Annexin B11	24	4	16.7
Tetraspanin 39D	13	1	7.7
Golgi complex-localized glycoprotein 1	17	0	0.0
Mucin 12Ea	18	1	5.6
Eps15 homology domain containing protein-binding protein 1	14	1	7.1
vanin-like	19	1	5.3
Leucine-rich repeat protein	21	1	4.8
croquemort	21	2	9.5
uninflatable	19	0	0.0

3.2 Further investigation

3.2.1 DIP ζ acts in multiple neuron classes to maintain AB circuit asymmetry

To further refine in which neuronal population DIP ζ is required for AB asymmetry, the before used driver combination *;per-GAL4,R72A10 LexA,LexAopGFP/CyO;TM2/TM3* (*SA^{uni}-GAL4*) and *;R72A10-LexA,LexAopGFP/CyO; R70H05-GAL4/TM2* (*vΔ-GAL4*), here referred to as *SA^{uni}-GAL4/vΔ-GAL4*, was complemented by additional neuron-type-specific GAL4 drivers that separately target either SA^{uni} (*;per-GAL4, R72A10-LexA,LexAopGFP/CyO;TM2/TM3*), vΔ (*;R72A10-LexA,LexAopGFP/CyO;R70H05-GAL4/TM2*) or SA^{bi} (*fas2^{Mz507}-GAL4; R72A10-LexA,LexAopGFP/CyO;*) neurons.

All experiments were conducted at 25°C and 29°C, since GAL4-dependent expression and consequently RNAi knockdown efficiency, increase with higher developmental temperature (Duffy, 2002). This approach was intended to maximize knockdown efficiency.

The control experiment (*empty-GAL4*) showed a moderate baseline level of bilateral projections at 25°C (13.8%, n = 29), whereas at 29°C this value increased to 23.4% (n = 47), indicating that elevated temperature alone increases wiring variability. Consistent with this observation, midline-merged AB phenotypes (**Figure 10**), hallmark indicators of reduced midline guidance fidelity, were also more frequent at 29°C, further supporting the interpretation that elevated developmental temperature compromises structural precision indipendently of gene-specific knockdown.

Knockdown of DIP ζ in SA^{uni} and vΔ neurons resulted in a phenotype rate of 27.3% (n = 33) at 25°C, which, as expected, increased to 41.7% (n = 36) at 29°C. When the knockdown was restricted to SA^{uni} neurons (**Figure 7**), the highest overall phenotype rate of the entire screen was observed at 25°C (44.4%, n = 18). Surprisingly, however, this effect decreased at 29°C to 20.8% (n = 24), suggesting that DIP ζ is required at an optimal level in SA^{uni} neurons and that excessive depletion of the protein at 29°C may reduce the occurence of phenotypes rather than enhance it.

In vΔ neurons (**Figure 8**), DIP ζ knockdown at 25°C had only a minor impact on AB circuit lateralization (7.1%, n = 14), whereas the stronger knockdown achieved at 29°C produced a markedly higher phenotype rate (41.4%, n = 29). These findings indicate that the partial reduction of DIP ζ in vΔ neurons can likely be compensated by other molecular mechanisms, while more severe depletion at elevated temperature surpasses this compensatory capacity and results substantially higher phenotype frequencies.

In sum, DIP ζ knockdown resulted in a clear and reproducible bilateral phenotype pattern across different driver lines although the levels to which DIP ζ is required are neuron class specific (**Figure 9**).

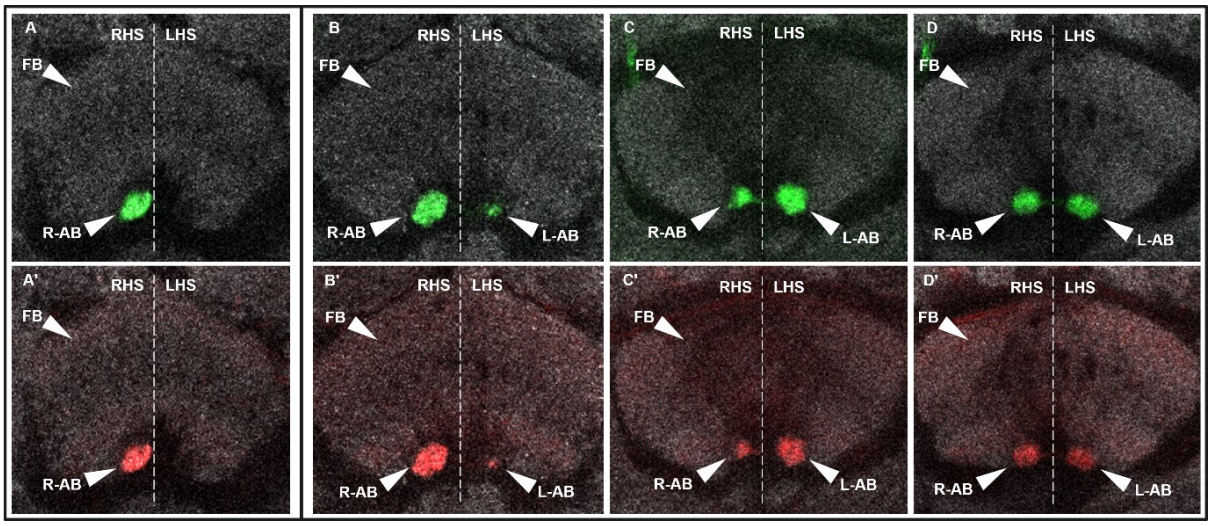

Figure 7. Phenotypic outcomes of DIP ζ knockdown in SA^{uni} neurons:
Representative confocal images show the projection phenotypes observed following RNAi-mediated knockdown of DIP ζ driven specifically in SA^{uni} neurons using *SA^{uni}-GAL4*. Panel **A** illustrates a wild-type-like phenotype, in which SA^{uni} neurons exhibit unilateral innervation restricted to the right Asymmetrical Body (R-AB). Panels **B-D** display different variations of bilateral Asymmetrical Body (AB) innervation that arise upon DIP ζ knockdown, with projections extending to both the right and left Asymmetrical Body (R-AB and L-AB). In panels **A-D**, SA^{uni} neuronal projections are visualized by green fluorescent protein (GFP). Corresponding panels **A'-D'**, show Fasciclin II (FasII) staining in red in the same brains, highlighting synaptic projections into the AB region and allowing direct comparison between neuronal morphology and synaptic organization. In all panels, arrows indicate the positions of the fan-shaped body (FB), the right Asymmetrical Body (R-AB), and the left Asymmetrical Body (L-AB), and the dashed vertical line marks the anatomical midline separating the right hemisphere (RHS) from the left hemisphere (LHS).
Abbreviations: AB = Asymmetrical Body; R-AB = right Asymmetrical Body; L-AB = left Asymmetrical Body; DIP ζ = Dpr-interacting protein ζ; RNAi = RNA interference; GFP = green fluorescent protein; FasII = Fasciclin II; FB = fan-shaped body; RHS = right hemisphere; LHS = left hemisphere; GAL4 = galactose-responsive transcription factor GAL4.

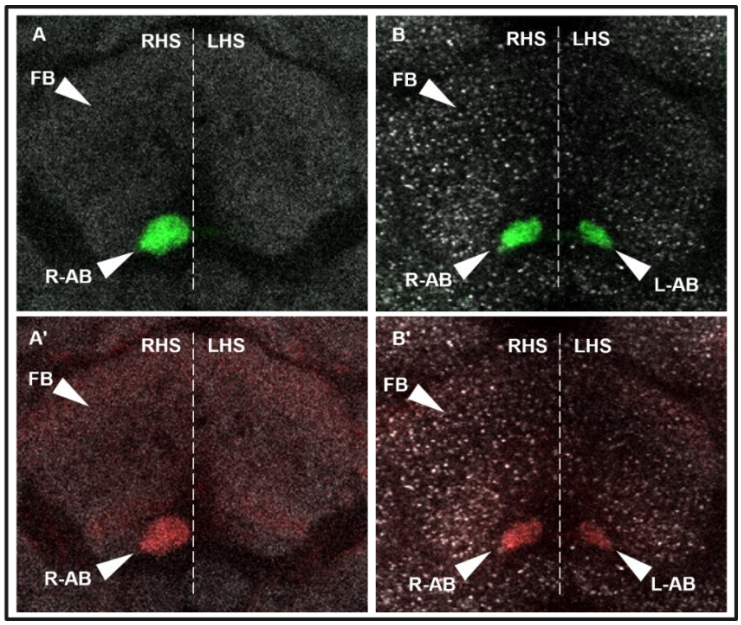

Figure 8. Phenotypic variation following DIP ζ RNAi knockdown in vΔ neurons:
Representative confocal images illustrate projection phenotypes observed after RNAi-mediated knockdown of DIP ζ driven specifically in vΔ neurons using *vΔ-GAL4*. Panel **A** shows a wild-type-like phenotype, characterized by unilateral innervation restricted to the right Asymmetrical Body (R-AB). Panel **B** displays a bilateral innervation phenotype, in which projections extend to both the right and left Asymmetrical Body (R-AB and L-AB) following reduction of DIP ζ. In panels **A and B**, SA^{uni} neuronal projections are visualized by green fluorescent protein (GFP). Corresponding panels **A' and B'** show Fasciclin II (FasII) staining in red in the same brains, highlighting synaptic projections into the Asymmetrical Body region and allowing comparison between neuronal morphology and synaptic organization. In all panels, arrows indicate the positions of the fan-shaped body (FB), the right Asymmetrical Body, and the left Asymmetrical Body, while the dashed vertical line marks the anatomical midline separating the right hemisphere (RHS) from the left hemisphere (LHS).
Abbreviations: AB = Asymmetrical Body; R-AB = right Asymmetrical Body; L-AB = left Asymmetrical Body; DIP ζ = Dpr-interacting protein ζ; RNAi = RNA interference; GFP = green fluorescent protein; FasII = Fasciclin II; FB = fan-shaped body; RHS = right hemisphere; LHS = left hemisphere; GAL4 = galactose-responsive transcription factor GAL4.

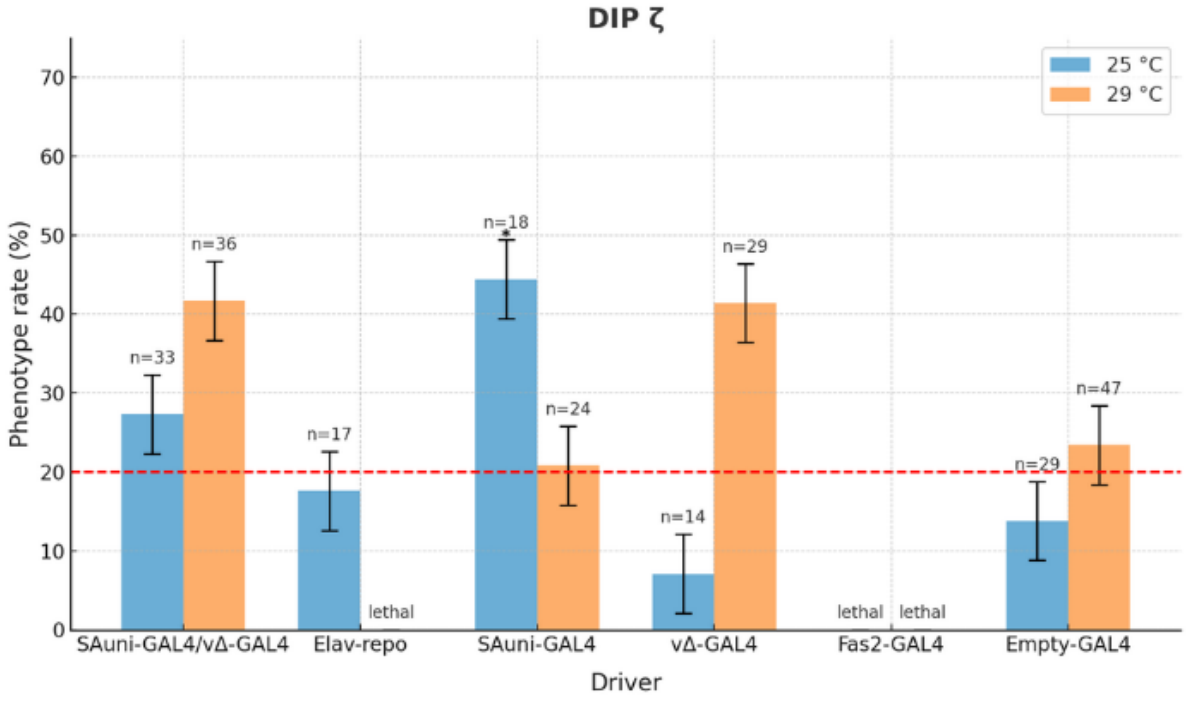

Figure 9. Phenotype rates following DIP ζ RNAi knockdown in different AB neuron populations at 25°C and 29°:

The bar graph quantifies the percentage of bilateral phenotypes observed following RNAi-mediated knockdown of DIP ζ driven by various neuron-type-specific GAL4 lines. Each GAL4 driver was tested at 25°C (blue bars) and at 29°C (orange bars) to assess potential temperature effects on RNAi efficiency and phenotype penetrance. The red dashed horizontal line marks the predefined threshold of 20% bilateral phenotypes used to distinguish biologically relevant effects from baseline variability. Error bars represent the standard deviation of the measured phenotype rates, and the number of analyzed brains (n) is indicated above each bar. Drivers that resulted in lethality under the respective conditions are indicated accordingly.

Abbreviations: AB = Asymmetrical Body; DIP ζ = Dpr-interacting protein ζ; n = number of analyzed brains; RNAi = RNA interference; GAL4 = galactose-responsive transcription factor GAL4.

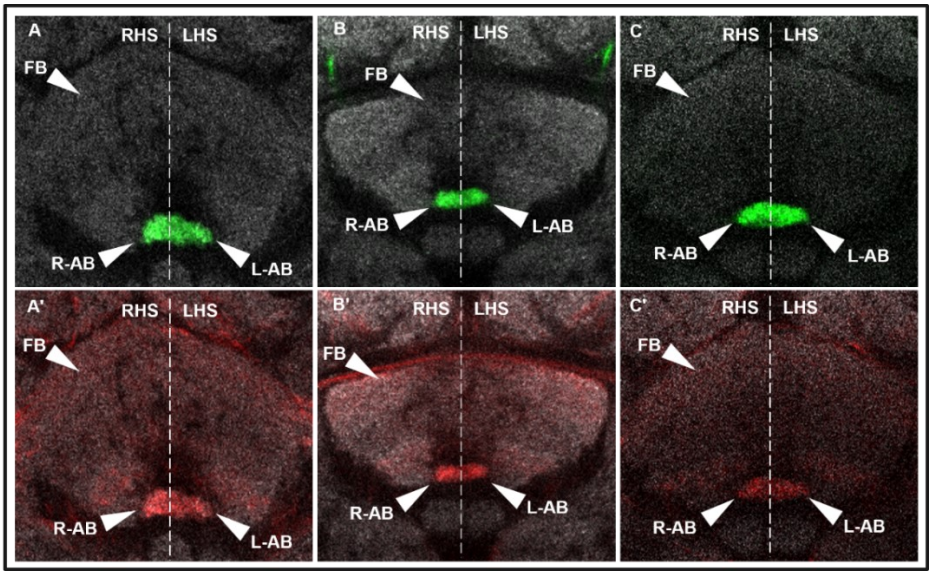

Figure 10. Midline-fused AB phenotypes observed at elevated developmental temperature (29°C):

Representative confocal images illustrate midline-fused Asymmetrical Body (AB) phenotypes observed following RNAi-mediated knockdown of DIP ζ at an elevated developmental temperature of 29°C. In these phenotypes, projections to the left and right Asymmetrical Body (L-AB and R-AB) extend across the anatomical midline and appear merged into a single, continuous structure. This midline-fused configuration was frequently observed under increased developmental temperature conditions. In panels **A-C**, SA^{uni} neuronal projections are visualized

by green fluorescent protein (GFP). Corresponding panels **A'-C'** show Fasciclin II (FasII) staining in red in the same brains, highlighting synaptic projections into the AB region and allowing direct comparison between neuronal morphology and synaptic organization. In all panels, arrows indicate the positions of the fan-shaped body (FB), the right Asymmetrical Body (R-AB), and the left Asymmetrical Body (L-AB), while the dashed vertical line marks the anatomical midline separating the right hemisphere (RHS) from the left hemisphere (LHS).
Abbreviations: AB = Asymmetrical Body; R-AB = right Asymmetrical Body; L-AB = left Asymmetrical Body; DIP ζ = Dpr-interacting protein ζ; GFP = green fluorescent protein; FasII = Fasciclin II; FB = fan-shaped body; RHS = right hemisphere; LHS = left hemisphere.

For 18w, the control experiment (*empty-GAL4*) showed no bilateral phenotypes at 25°C (0.0%, n = 21) and a low baseline at 29°C (11.8%, n = 17) (**Figure 11**).

Re-testing the 18w RNAi under the combined *SA^{uni}-GAL4/vΔ-GAL4* driver revealed a dramatic loss of the initial signal: the phenotype rate dropped from 50% (n = 26, **see Figure 6**) in the primary screen to 3.4% (n = 29) at 25°C (**Figure 11**), and statistical comparison confirmed that this value did not differ significantly from the control (**Table 5**). The phenotype rate at 29°C reached only 12.5% (n = 32) (**Figure 11**). These values were similar to the control at the higher temperature and indicate that the original high penetrance was not reproducible under the same experimental framework.

When the knockdown was restricted to SA^{uni} neurons alone, no bilateral phenotypes were observed at 25°C (0.0%, n = 35), and a modest rate appeared at 29°C (13.3.%, n = 30). Similarly, targeting SA^{bi} (*fas2-GAL4*) produced no phenotype rates at 25°C (0.0%, n = 18), but showed an elevated rate at 29°C (23.3%, n = 43). Knockdown in vΔ neurons yielded no phenotypes at 25°C (0.0%, n = 21), but a strong increase at 29°C (35.4%, n = 48) (**Figure 11**).

Overall, the rescreen demonstrates that the large effect seen for 18w in the initial screen is not robust: phenotype frequencies are largely absent at 25°C and, where elevated at 29°C, mirror a general temperature-dependent increase observed across multiple lines. Therefore, 18w is most likely not an important factor in AB lateralization in *D. melanogaster*. Consequently, 18w was excluded from further experiments and DIP ζ remained as the only strong candidate for detailed developmental and functional follow-up analyses.

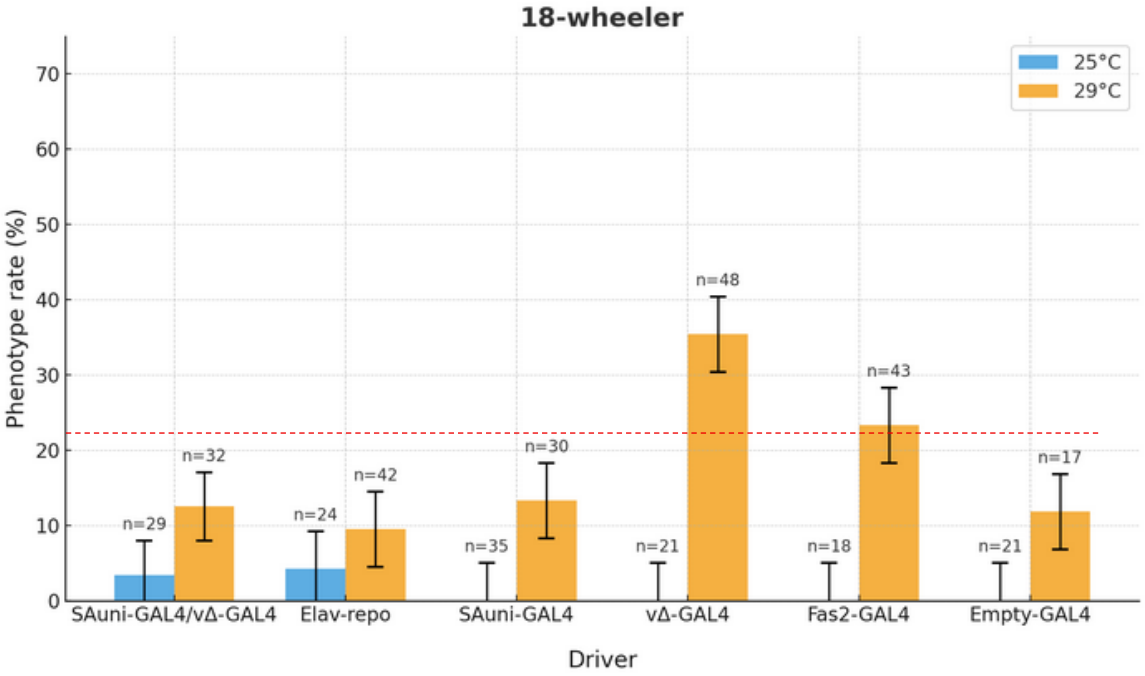

Figure 11. Phenotype rates following 18w RNAi knockdown across different driver lines at 25°C and 29°:
The bar graph quantifies the percentage of bilateral phenotypes observed following RNAi-mediated knockdown of 18w using different neuron-type-specific GAL4 drivers. Each GAL4 driver was tested at 25°C (blue bars) and at 29°C (orange bars) to evaluate potential temperature-dependent effects on RNAi efficiency and phenotype penetrance. The red dashed horizontal line marks the predefined threshold of 20% bilateral phenotypes used to distinguish biologically relevant effects from baseline variability. Error bars represent the standard deviation of the measured phenotype rates, and the number of analyzed brains (n) is indicated above each bar.
Abbreviations: 18w = 18-wheeler; n = number of analyzed brains; RNAi = RNA interference; GAL4 = galactose-responsive transcription factor GAL4.

Table 5. Results of the secondary RNAi screen for DIP ζ and 18w:
N = number of total brains analyzed per line; Percentages rounded to one decimal place.

gene	T (°C)	Driver	N	N (phenotypes)	% (phenotypes)	Test used	X^2	p	p (Bonferroni-corrected)
DIP ζ	25°C	*SA^{uni}-GAL4/vΔ-GAL4*	33	9	27.3%	Chi²	0.98	0.323	1.0
		Elav-repo	17	3	17.6%	Chi²	0.00	1.000	1.0
		SA^{uni}-GAL4	18	8	44.4%	Chi²	**3.99**	**0.046**	0.228
		vΔ-GAL4	14	1	7.1%	Chi²	0.02	0.897	1.0
		Fas2-GAL4	-	-	-	-	-	-	-
		Empty-GAL4	29	4	13.8%	-	-	-	-
	29°C	*SA^{uni}-GAL4/vΔ-GAL4*	36	15	41.7%	Chi²	2.37	0.124	0.619
		Elav-repo	-	-	-	-	-	-	-
		SA^{uni}-GAL4	24	5	20.8%	Chi²	0.00	1.000	1.0
		vΔ-GAL4	29	12	41.4%	Chi²	1.96	0.162	0.808
		Fas2-GAL4	-	-	-	-	-	-	-
		Empty-GAL4	47	11	23.4%	-	-	-	-
18w	25°C	*SA^{uni}-GAL4/vΔ-GAL4*	29	1	3.4%	Chi²	0.00	1.000	1.0
		Elav-repo	24	1	4.2%	Chi²	0.00	1.000	1.0
		SA^{uni}-GAL4	35	0	0.0%	Chi²	-	-	-
		vΔ-GAL4	21	0	0.0%	Chi²	-	-	-
		Fas2-GAL4	18	0	0.0%	Chi²	-	-	-
		Empty-GAL4	21	0	0.0%	-	-	-	-
	29°C	*SA^{uni}-GAL4/vΔ-GAL4*	32	4	12.5%	Chi²	0.00	1.000	1.0
		Elav-repo	42	4	9.5%	Chi²	0.00	1.000	1.0
		SA^{uni}-GAL4	30	4	13.3%	Chi²	0.00	1.000	1.0
		vΔ-GAL4	48	17	35.4%	Chi²	2.35	0.125	0.627
		Fas2-GAL4	43	10	23.3%	Chi²	0.42	0.519	1.0
		Empty-GAL4	17	2	11.8%	-	-	-	-

3.2.2 Early vs. Late developmental requirements of DIP ζ in AB circuit lateralization

Bilateral innervation of SA^{uni} neurons can arise through two distinct mechanisms: either the initial remodeling of SA^{uni} fails, or the remodeling occurs but is not maintained afterwards. To determine how bilateral innervation develops when DIP ζ expression is downregulated in SA^{uni} neurons, pupal brains were dissected at 50h APF. This developmental stage was chosen because SA^{uni} remodeling is fully completed at 50h APF, so any phenotypes observed at this stage indicate a disruption of the initial remodeling process.

For this, DIP ζ was downregulated in SA^{uni} and vΔ neurons together and separately in afferent SA^{uni} neurons at 25°C. With the combined *SA^{uni}-GAL4/vΔ-GAL4* driver, I observed 22.2% (n=9) bilateral phenotypes in pupal brains (**Figure 12**) and this level was maintained into adulthood (n=32; 28.1%), where I dissected adult brains from the same genetic cross under identical conditions (**Figure 13**). This finding strongly suggests that DIP ζ is required in vΔ and SA^{uni} neurons to form a lateralized AB circuit from a bilateral ground state.

In contrast, when DIP ζ was downregulated in SA^{uni} neurons alone, no bilateral phenotypes were observed in pupal brains. In adult brains of the same cross, I got a bilateral phenotype rate of 13.3% (n = 15) (**Figure 13**).

This indicates that in SA^{uni} neurons, the phenotype emerges later, either during late pupal stages or shortly after eclosion. This points towards a role of DIP ζ in SA^{uni} neurons for the maintenance of the remodeled circuit.

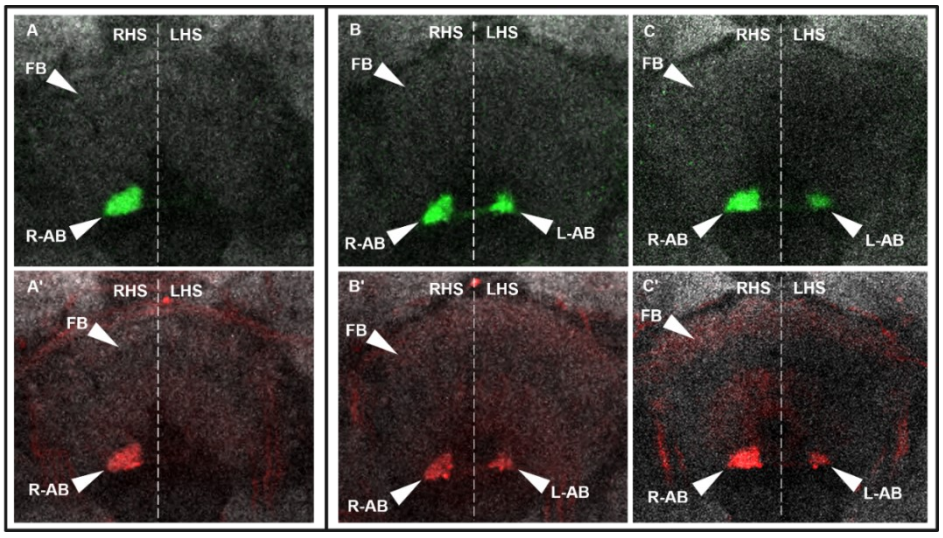

Figure 12. Phenotypic variation following DIP ζ RNAi knockdown at 50h APF:
Representative confocal images illustrate projection phenotypes observed at 50h after puparium formation (APF) following RNAi-mediated knockdown of DIP ζ driven by the combined *SA^{uni}-GAL4/vΔ-GAL4* driver. Panel **A** shows

a wild-type-like phenotype, characterized by unilateral innervation restricted to the right Asymmetrical Body (R-AB). Panels **B and C** display bilateral innervation phenotypes, in which projections extend to both the right and left asymmetrical bodies (R-AB and L-AB) upon reduction of DIP ζ. In panels **A-C**, SA^{uni} neuronal projections are visualized by green fluorescent protein (GFP). Corresponding panels **A'-C'** show Fasciclin II (FasII) staining in red in the same brains, highlighting synaptic projections into the AB region and allowing comparison between neuronal morphology and synaptic organization. In all panels, arrows indicate the positions of the fan-shaped body (FB), the right Asymmetrical Body (R-AB), and the left Asymmetrical Body (L-AB), while the dashed vertical line marks the anatomical midline separating the right hemisphere (RHS) from the left hemisphere (LHS).
Abbreviations: h = hours; APF = after puparium formation; AB = Asymmetrical Body; R-AB = right Asymmetrical Body; L-AB = left Asymmetrical Body; DIP ζ = Dpr-interacting protein ζ; GFP = green fluorescent protein; FasII = Fasciclin II; FB = fan-shaped body; RHS = right hemisphere; LHS = left hemisphere; RNAi = RNA interference; GAL4 = galactose-responsive transcription factor GAL4.

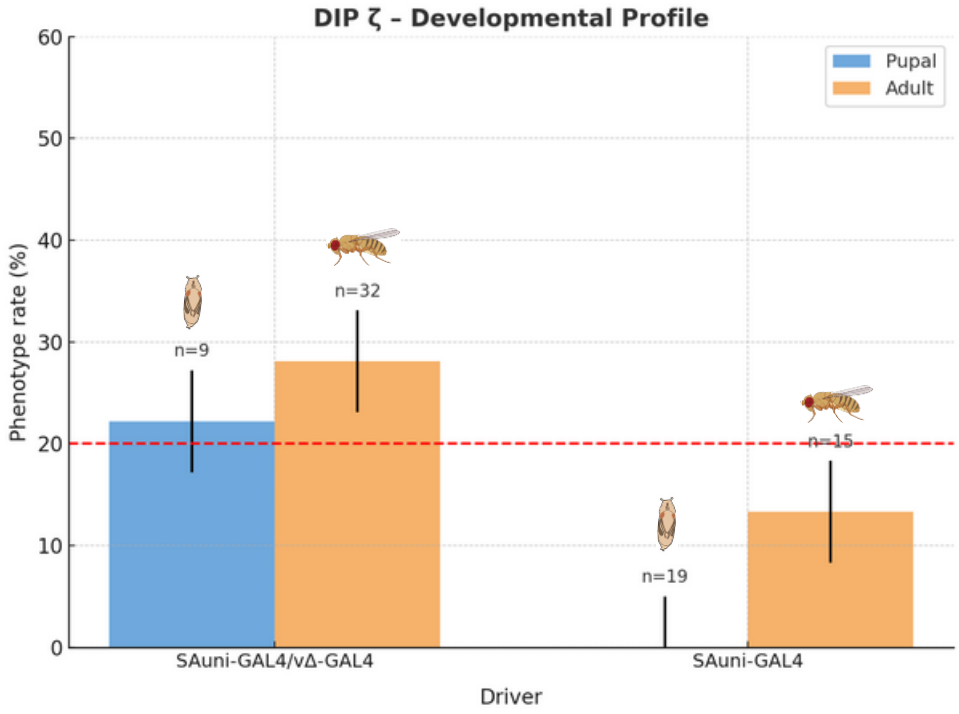

Figure 13. Phenotype rate for DIP ζ RNAi at 50h APF and adults from the same cross:
The bar graph compares bilateral phenotype rates observed at 50h after puparium formation (APF) and in adult brains following RNAi-mediated knockdown of DIP ζ from the same genetic crosses. The blue bars represent the percentage of bilateral phenotypes detected in pupal brains, whereas the orange bars represent the corresponding phenotype rates measured in adult brains. Knockdown was driven either by the combined *SA^{uni}-GAL4/vΔ-GAL4* driver or by *SA^{uni}-GAL4* alone. The red dashed horizontal line marks the predefined threshold of 20% bilateral phenotypes, which was used to distinguish biologically relevant effects from baseline variability observed in wild-type controls. Error bars indicate the standard deviation, and the number of analyzed brains (n) is indicated above each bar.
Abbreviations: AB = Asymmetrical Body; h = hours; APF = after puparium formation; DIP ζ = Dpr-interacting protein ζ; n = number of analyzed brains; RNAi = RNA interference; GAL4 = galactose-responsive transcription factor GAL4.

4. Discussion

4.1 General overview and key findings

Brain asymmetry is a shared organizational principle of the bilaterian CNS and is thought to enhance processing efficiency by reducing hemispheric redundancy and supporting specialized behavioural outputs (Rogers et al., 2013; Postema et al., 2019). In this study, a targeted RNAi screen was performed to identify novel genes required for the establishment of central brain asymmetry in *D. melanogaster*. Twenty different genes were knocked down in AB-afferent SA^{uni} neurons and AB-efferent vΔ neurons using the combined *SA^{uni}-GAL4/vΔ-GAL4* driver. Bilateral AB innervation, a deviation from the wild-type right-biased projection pattern, was used as the phenotypic readout.

Two analyzed genes exceeded the predefined threshold of 20% bilateral projections in the initial screen: 18-wheeler (18w) and Dpr-interacting protein ζ (DIP ζ). However, in a rescreen under identical conditions, the 18-wheeler phenotype was not reproducible, consistent with known variability in RNAi knockdown efficiency and temperature-sensitive developmental processes (Dietzl et al., 2007). In contrast, DIP ζ knockdown consistently reduced neuronal asymmetry, confirming it as a robust regulator of AB asymmetry.

Neuron-specific rescreening revealed that the strength and timing of the phenotype depended on the neuronal population targeted. DIP ζ knockdown in exclusively SA^{uni} neurons produced a high bilateral phenotype rate in adults at 25°C, whereas no bilateral phenotypes were detected at the pupal stage (50h APF). This indicates that the phenotype in this condition is not established during the initial remodeling phase but instead emerges later, most likely during late pupal development or early adulthood, consistent with a defect in maintaining rather than establishing asymmetry.

Conversely, the combined *SA^{uni}-GAL4/vΔ-GAL4* driver yielded bilateral projections already in pupae, and this phenotype persisted into adulthood. At first glance, this pattern suggests that concurrent loss of DIP ζ in afferent and efferent neurons disrupts the remodeling process itself. However, vΔ neurons are known to innervate the AB only after SA^{uni} remodeling has been completed (Markovitsch et al., 2025), meaning that the early pupal phenotype cannot be explained by a remodeling defect in vΔ neurons. Instead, the more parsimonious interpretation is that DIP ζ knockdown in SA^{uni} neurons is sufficient to destabilize the

remodeling process, whereas knockdown in vΔ neurons contributes an additional, earlier-acting maintenance defect that becomes detectable only when both populations are targeted. This interpretation implies that the critical temporal window of DIP ζ function may differ between these neuron classes, and that earlier pupal stages than 50h APF will be required to precisely determine when the phenotype first arises. Thus, DIP ζ is most likely required for maintaining the asymmetry of the AB circuit.

Taken together, these findings identify DIP ζ as a novel molecular regulator of central brain lateralization in *D. melanogaster* that is required in afferent and efferent neurons of the AB circuit to ensure the maintenance of the unilateral projection pattern of SA^{uni} neurons.

4.2 Developmental dynamics of AB asymmetry

The developmental timing of the observed DIP ζ phenotypes provides a tentative but informative indication of when this gene contributes to the establishment of AB lateralization. In the wild-type brain, the AB circuit asymmetry is established by a remodeling step from a symmetrical ground state. During metamorphosis, SA^{uni} neurons initially project bilaterally, and the left-side projections are subsequently removed through a remodeling process that occurs between approximately 35-40 hours after puparium formation (Sakamura et al., 2023). This pruning phase coincides with widespread, hormone-dependent structural reorganization in the central nervous system, where larval neuronal arbors/branches are selectively eliminated and replaced with adult-specific circuitry (Yu & Schuldiner, 2014; Truman & Riddiford, 2023). Recent work has shown that AB lateralization specifically depends on asymmetrically acting guidance cues during this pupal window: Netrin-B signaling, for example, biases the stabilization of right-hemispheric SA^{uni} projections and promotes retraction of axons on the left side (Lapraz et al., 2023).

In this context, the DIP ζ phenotypes reveal when the gene acts within this remodeling sequence. Upon DIP ζ knockdown in both SA^{uni} and vΔ neurons (*SA^{uni}-GAL4/vΔ-GAL4*), bilateral innervation was already detectable at ≈ 50h APF, indicating a failure of the left-side retraction or stabilization during the remodeling phase. However, when DIP ζ was knocked down in SA^{uni} neurons alone, no bilateral phenotypes were present at the same pupal time point, and bilateral innervations were observed in adults. This discrepancy suggests that the timing of DIP

ζ function differs between neuron classes: the SA^{uni} driver (*per-GAL4*) is active early, whereas *vΔ-GAL4* is known to begin expression only later in metamorphosis. Thus, the combined driver likely reduces DIP ζ in both cell populations during different critical pruning periods, while the SA^{uni}-only knockdown may not be sufficient at that stage to disrupt pruning, and instead affects later stabilization or re-growth.

Taken together, the developmental data support a model in which DIP ζ is required in two distinct phases and in two different neuronal populations, but always in the context of maintaining an already remodeled state rather than initiating it.

In SA^{uni} neurons, DIP ζ appears to function during the late pupal period, after the major remodeling events (≈ 50h APF), where it helps preserve the correctly pruned, right-sided projection pattern. In the absence of DIP ζ, these neurons may fail to maintain the remodeled architecture, allowing left-sided terminals to persist or re-emerge.

In vΔ neurons, DIP ζ is likewise required for the stability of the mature circuit. Because vΔ-SA^{uni} synaptic contacts form after SA^{uni} pruning has already taken place, DIP ζ in vΔ neurons cannot influence the pruning phase itself, but instead contributes to maintaining the established tight-hemisphere connectivity during late pupal and early adult stages.

Overall, these observations suggest that DIP ζ functions primarily as a stabilizer („sustainer“) of the remodeled AB circuit, ensuring that the right-sided wiring pattern, once established through earlier pruning, is preserved and protected from later destabilization or aberrant regrowth.

This model is compatible with the observation that AB asymmetry is generated not by asymmetric initial growth, but by selective pruning and stabilization during development (Pascual et al., 2004; Veverytsa & Allan, 2013). It also explains why the SA^{uni}-alone phenotype appears only in adult brains: the remodeling may initially proceed correctly, but without DIP ζ, the resulting unilateral projection is not stably maintained and subsequently becomes bilateral.

To further clarify the temporal and cell-type-specific functions of DIP ζ, future experiments should incorporate earlier pupal time points, such as 35-45h APF, to determine whether left-side left-side pruning initially occurs normally, and employ temporally controlled knockdown

systems such as GAL80^ts to restrict RNAi induction to either early or late metamorphic stages. Complementary experiments involving live imaging of SA^{uni} axon dynamics during remodeling would also help to visualize whether DIP ζ primarily influences the onset of pruning, the subsequent stabilization of right-side projections, or a combination of both processes. Together, these approaches will refine the mechanistic understanding of how SA^{uni} and vΔ neuron populations contribute to the establishing and maintaining AB lateralization.

4.3 Dpr-DIP-mediated cell-surface recognition in nervous system development

Developmental processes that involve selective pruning and stabilization of neuronal connections require molecular mechanisms that can distinguish transient from persistent contacts at a local scale. In the *Drosophila* nervous system, one such mechanism is provided by the Defective proboscis response (Dpr) and Dpr-interacting protein (DIP) families, which together form a large immunoglobulin superfamily-based network of cell-surface recognition molecules (Özkan et al., 2013; Carillo et al., 2015). Dprs and DIPs engage in heterophilic, trans-synaptic interactions that promote selective adhesion between neuronal partners, thereby biasing which connections are retained during circuit refinement (Tan et al., 2015; Cosmanescu et al., 2018).

Unlike long-range guidance cues that direct axons toward target regions, Dpr-DIP interactions act locally at sites of contact and primarily influence synaptic matching and stabilization (Carillo et al., 2015; Ashley et al., 2019). This distinction has been demonstrated most clearly in the visual system, where highly cell-type- and layer-specific expression of Dpr and DIP genes ensures precise connectivity between afferent neurons and specific postsynaptic target neuron populations (Tan et al., 2015; Cosmanescu et al., 2018). Loss of individual Dpr-DIP pairs in these circuits leads to inappropriate partner choice or reduced synapse stability, indicating a role in refining connectivity rather than initiating axon outgrowth (Carrillo et al., 2015; Ashley et al., 2019).

Comparable functions have been described in other developmental contexts. In the mushroom body, Dpr-DIP interactions contribute to compartment-specific wiring by promoting selective recognition between synaptic partners during circuit assembly and remodeling (Bornstein et al., 2021). Structural and biophysical studies further revealed that

specificity within the Dpr-DIP network arises from subtle differences in Ig-domain interfaces, allowing a relatively small gene family to generate a broad range of selective interactions (Cheng et al., 2019; Sergeeva et al., 2020). Recent work has added an additional regulatory layer by showing that cis interactions between Dprs and DIPs on the same membrane can modulate trans binding and fine-tune adhesive strength, thereby influencing whether contacts are stabilized or remain transient (Morano et al., 2025).

In this context, individual DIP family members can be understood as context-dependent stabilizers whose developmental impact depends on their expression timing, cellular localization, and available binding partners in a given circuit.

4.4 Molecular interpretation, biological significance, and mechanistic hypotheses

The identification of DIP ζ as a regulator of AB asymmetry places this protein within the Dpr-DIP immunoglobulin superfamily network. Within this family, selective pairing between individual Dprs and DIPs underlies functional specificity. Biochemical interactome mapping shows that DIP ζ binds to a specific subset of Dpr proteins (Özkan et al., 2013; Cosmanescu et al., 2018). However, no published data currently demonstrate DIP ζ expression in SA^{uni}or vΔ neurons, and existing expression reports place DIP ζ in restricted neuronal populations such as medulla neurons of the optic lobe and subsets of peripheral motor and sensory neurons (Tan et al., 2015; FlyBase, accessed 2025). The bilateral AB phenotype observed in this study therefore implies that at least one of these Dpr partners must be expressed in AB-associated neurons, even though the identity and cellular location of the relevant Dpr remain unknown. This represents a direct and experimentally tractable question for future work.

The developmental timing of the DIP ζ phenotype provides insight into its mechanistic role. In wild-type development, SA^{uni} neurons initially projec bilaterally and subsequently prune their lef-sided branches during the pupal remodeling window (≈ 35-40h APF) before stabilizing the right-sided projection (Sakamura et al., 2023; Yu & Schuldiner, 2014; Truman & Riddiford, 2023). The key observation in this study is that the knockdown of DIP ζ in SA^{uni} and vΔ neurons together produces bilateral phenotypes already at ≈ 50h APF, whereas the knockdown in SA^{uni} alone produces bilateral phenotypes only in adults. Because vΔ neurons innervate the AB only

after SA^{uni} pruning has been completed (Markovitsch et al., 2025), the early pupal phenotype cannot be explained by a defect in vΔ neurons acting during the pruning phase.

A more coherent interpretation is that DIP ζ is required for stabilizing right-sided connections during or immediately after pruning, and that reducing DIP ζ expression on both sides of the prospecive synapse (SA^{uni} and vΔ/target neurons) lowers overall adhesion strength sufficiently to reveal a stabilization defect already during pupal stage. When DIP ζ is reduced only in SA^{uni} neurons, no bilateral phenotype is observed at the same pupal stage, and instead bilateral innervation appears only in adults, suggesting that remodelling may initially proceed correctly, but right-sided stabilization later fails, allowing re-extension or loss of hemispheric specificity. In this model, DIP ζ knockdown in both cell populations reduces the robustness of right-side stabilization below a critical threshold earlier in metamorphosis, producing the earlier and more penetrant pupal phenotype.

This interpretation resolves the timing discrepancy while remaining consistent with the known developmental sequence of the AB circuit. Is also aligns with prior findings that the AB asymmetry is generated not by asymmetric initial growth but through selective pruning and subsequent stabilization (Pascual et al., 2004; Veverytsa & Allan, 2023). DIP ζ and its Dpr partners would, in this scenario, provide the adhesion-based recognition cues needed to consolidate right-hemispheric projections, while left-side branches lacking appropriate adhesive matches remain transient and are eliminated.

Taken together, the results support a mechanistic model in which DIP ζ operates as part of a trans-synaptic adhesion-based recognition system, ensuring that right-side synapses formed by SA^{uni} neurons are selectively stabilized, while left-side connections remain transient and are eliminated. In the absence of DIP ζ, this stabilization fails, leading to the persistence or recovery of left-side projections, and ultimately, bilateral AB innervation.

4.5 Temperature effects and midline phenotypes

A striking observation in this study was the strong temperature dependence of AB phenotypes. When flies were raised at 29°C, bilateral and midline-fused Asymmetrical Body (AB) phenotypes occurred far more frequently than at 25°C, not only in DIP ζ knockdown lines but also in the genetic controls. This clearly demonstrates that developmental temperature itself

is a major environmental factor affecting neuronal wiring fidelity and gene expression dynamics.

In *Drosophila*, the GAL4/UAS system exhibits temperature-dependent transcriptional efficiency: increasing rearing temperature from 25°C to 29°C substantially enhances GAL4 activity and therefore intensifies RNAi-induced gene silencing (Brand & Perrimon, 1993). However, higher temperatures also accelerate metamorphosis, shorten critical remodeling phases, and alter neuronal physiology in ways that can non-specifically affect circuit formation (Chen et al., 2012). Importantly, developmental temperature has been shown to modify synapse number and axonal branching, leading to variable partner choice fidelity in the fly brain (Kiral et al., 2021; Peng et al., 2007). Thus, the stronger phenotypes observed at 29°C likely result from a combined effect of enhanced RNAi efficiency and increased developmental stress, which is known to reduce the stability and precision of neural wiring (Kiral et al., 2021).

The frequent midline-fused ABs observed at 29°C are especially noteworthy. Such midline fusion phenotypes are characteristic of impaired axon guidance and arise when canonical midline signaling pathways, most prominently Slit-Robo and Netrin-Frazzled, are perturbed/disturbed (Kidd et al., 1999; Garbe & Bashaw, 2007). These systems normally maintain left-right segregation by providing repulsive and attractive cues during CNS development. Temperature-induced changes in protein folding, expression timing, or intracellular signaling could weaken these cues, resulting in atypical midline crossing. In addition, loss of DIP ζ may increase this effect by destabilizing adhesion-based recognition between AB-associated neurons, since DIPs and Dprs interact with multiple signaling complexes and other adhesion molecules (Carrillo et al., 2015).

Another explanation for the temperature-dependent enhancement of bilateral and midline phenotypes involves the timing of driver activity. The *vΔ-GAL4* driver becomes active relatively late during metamorphosis, around 40 hours after puparium formation (APF), whereas the *SA^{uni}-GAL4* driver (*per-GAL4*) is active earlier. At higher temperature, these developmental stages are temporally compressed, and the window for RNAi expression may partially overlap or shift relative to the critical remodeling phase. As a result, gene knockdown may occur too late or too transiently in certain cell types, leading to asynchronous effects between afferent (SA^{uni}) and efferent (vΔ) neurons. Such temporal mismatches could produce secondary or

compensatory phenotypes, for instance, SA^{uni} projections retract normally, but subsequently regrow to the left AB due to altered vΔ signaling or instability in target recognition.

The elevated bilateral rates in the *empty-GAL4* control lines at 29°C further support the view that temperature itself introduces wiring variability. Similar temperature-induced effects on neural connectivity have been documented in *Drosophila* visual circuits, where increased developmental temperature correlates with greater variability in synaptic structure and partner matching (Peng et al., 2007). Consequently, phenotypes observed under these conditions should be interpreted as the combined outcome of stronger gene knockdown and reduced developmental precision.

To disentangle gene-specific from temperature-dependent effects, future experiments should employ temporally controlled expression systems such as tub-GAL80^ts to restrict RNAi induction to defined developmental stages. Alternatively, cell-type-specific CRISPR-based knockdown strategies could achieve strong gene suppression without the need for elevated temperatures, thereby avoiding the developmental confounds associated with 29°C. Overall, while high temperature remains a practical tool to enhance GAL4-UAS activity, it also imposes biological perturbations that reduce wiring fidelity, emphasizing that genetic and environmental factors jointly influence the development of structural brain asymmetry.

4.6 Methodological reflections and limitations of the study

While this study successfully identified Dpr-interacting protein ζ (DIP ζ) as a potential regulator of structural lateralization in the *Drosophila* brain, several methodological constraints must be considered when interpreting the results. These limitations concern both the experimental tools used, particularly RNA interference (RNAi) and the GAL4/UAS system, and the biological complexity of the developmental process being studied.

RNAi efficiency and specificity

A major limitation of RNAi-based screening is its variable efficiency and potential for off-target effects. Even under standardized conditions, RNAi constructs can produce inconsistent knockdown across tissues due to differences in transgene insertion sites, local chromatin context, or secondary structure of the target mRNA (Dietzl et al., 2007; Perkins et al., 2015). The dramatic discrepancy observed for 18-wheeler (18w), which displayed a 50% phenotype

rate in the initial screen but only 3% in the rescreen, illustrates this variability. Such a drop likely reflects differences in RNAi potency/power between generations or environmental modulation of GAL4 activity, but could also indicate that the original phenotype was due to a non-specific effect or stochastic variability in circuit remodeling. This variability is not unusual in developmental systems where timing, temperature, and gene expression are tightly coupled. Reproducibility could be improved through validation with multiple independent RNAi constructs, CRISPR-generated null mutants, or genetic rescue experiments (Port et al., 2020).

Driver specificity and temporal expression

Another methodological consideration is the specificity and timing of GAL4 driver expression. The *SA^{uni}-GAL4/vΔ-GAL4* combination was used to target both afferent and efferent neurons of the AB, but the drivers differ in activation time, *SA^{uni}-GAL4* (*per-GAL4*) is active early in development, whereas *vΔ-GAL4* becomes active around 40 hours after puparium formation (APF). This temporal offset complicates interpretation because the onset of knockdown does not necessarily coincide with the critical remodeling phase in both cell populations. As a result, the bilateral phenotypes observed might reflect asynchronous knockdown effects rather than direct trans-synaptic consequences. Incorporating temporal control, such as *tub-GAL80^ts* to restrict RNAi activation to defined windows, or using intersectional approaches (e.g., *split-GAL4*) could address this issue (Pfeiffer et al., 2010; Luan et al., 2006).

Quantification and interpretation of phenotypes

Phenotypic scoring in this study was based on manual classification of confocal images, which, while sufficient for detecting qualitative differences, introduces observer bias and limits quantitative precision. Some subtle variations, such as partial bilateral projections or asymmetric arbor sizes, may not have been captured by binary classification. Automated image analysis pipelines and volumetric segmentation tools, for instance in Fiji or Imaris, could provide more objective quantification of asymmetry (Schindelin et al., 2012). Additionally, integrating volumetric measurements or axon projection ratios could help distinguish between mild and severe phenotypes, offering a more nuanced view of DIP ζ function.

Temperature as a confounding factor

The use of elevated temperature (29°C) to enhance GAL4 activity also introduces confounding effects. As discussed in section 4.4, developmental temperature affects both gene expression

and neural wiring fidelity (Peng et al., 2007; Kiral et al., 2021). The high bilateral phenotype rates observed in control flies at 29°C emphasize that some of the observed effects likely arise from temperature-induced instability rather than genuine gene-specific mechanisms.

Sample size and statistical power

Although the observed trends were consistent, sample sizes were limited for some conditions (particularly the pupal dissections), which reduces statistical power and increases susceptibility to random variation. This may partly explain the inconsistent phenotype rates between developmental stages or replicates. Increasing the number of analyzed brains per group and performing statistical corrections for multiple comparisons (e.g., Bonferroni correction) will improve robustness in future screens.

Functional readouts and behavioural validation

This study focused exclusively on anatomical asymmetry without assessing potential functional consequences. Since AB lateralization has been linked to long-term memory and orientation behaviors (Pascual et al., 2004; Strauss, 2002), correlating structural phenotypes with behavioral assays, such as memory performance, orientation choice, or locomotor bias, would provide a crucial link between anatomy and function.

4.7 A model for DIP ζ-dependent stabilization of asymmetric AB wiring

The findings of this study suggest that Dpr-interacting protein ζ (DIP ζ) contributes to the maintenance of Asymmetrical Body (AB) laterality by stabilizing selective neuronal contacts during metamorphosis. Rather than acting as a long-range guidance cue, DIP ζ appears to function locally at the membrane surface of AB-associated neurons, where it engages in heterophilic binding with members of the Dpr family. DIPs and Dprs form well-characterized cell-adhesion complexes whose extracellular Ig-domains mediate selective recognition and whose intracellular regions associate with scaffolding components implicated in synaptic organization (Özkan et al., 2013; Carrillo et al., 2015; Ashley et al., 2019; Bornstein et al., 2021). Although the exact intracellular pathways linking DIP/Dpr adhesion to structural stabilization remain incompletely understood, available evidence supports a role for these complexes in reinforcing appropriate partner contacts in multiple CNS circuits.

In the wild-type scenario (**Figure 14A**), SA^{uni} neurons initially project bilaterally, but left-side branches are removed during early pupal remodeling, resulting in stable right-hemisphere projections (Pascual et al., 2004; Lapraz et al., 2023). Within this context, DIP ζ is positioned in the plasma membrane of SA^{uni} and vΔ or other AB-adjacent neurons, forming adhesive contacts with one or more of its known partners — Dpr6, Dpr13, Dpr16, Dpr19 or Dpr20 (Özkan et al., 2013). These interactions provide molecular selectivity that can, in principle, reinforce synaptic or pre-synaptic specializations on the right AB. Where complementary Dpr partners are not present, such as on the left AB, weaker adhesion may contribute to the removal or failure to stabilize those contacts. This interpretation aligns with findings in the visual system, where DIP-Dpr interactions help match specific neuron types and mediate the stabilization of appropriate contacts (Carrillo et al., 2015; Ashley et al., 2019).

The close-up schematic in **Figure 14** illustrates this concept: DIP ζ and Dpr molecules occupy opposing neuronal membranes within right-side AB microdomains, forming heterophilic adhesive pairs that confer molecular selectivity. Their extracellular Ig-domains mediate this recognition, while their intracellular regions, as suggested by studies in other circuits, are positioned to interact with synaptic scaffolds (Ashley et al., 2019; Bornstein et al., 2021), potentially influencing the persistence of newly stabilized contacts. Although the precise intracellular mechanisms in AB-associated neurons remain unknown, this arrangement provides a plausible structural basis for how DIP ζ supports the asymmetric maintenance of projections.

In DIP ζ knockdown flies (**Figure 14B**), this selective adhesion interface is weakened. Without sufficient DIP ζ at the membrane, right-side contacts may fail to consolidate effectively, allowing SA^{uni} axons to retain or re-extend projections toward the left AB. Because *SA^{uni}-GAL4* is active early, while *vΔ-GAL4* becomes active later (≈ 40h APF), the timing of DIP ζ loss likely differs between the two neuron classes. This temporal mismatch provides a coherent explanation for the developmental results: SA^{uni} neurons may remodel normally at first, but later destabilization, arising once vΔ neurons begin expressing RNAi, could permit regrowth or retention of left-side branches. The consistent and robust phenotype observed only when both drivers are active supports the idea that DIP ζ is required in both neuron populations, albeit at different developmental phases.

This interpretation also harmonizes with known pruning and stabilization pathways. During metamorphosis, SA^{uni} remodeling is guided by pruning cues such as Netrin-B/Frazzled (Lapraz et al., 2023) and stabilized by adhesion molecules including Fasciclin II (Markovitsch et al., 2025). DIP ζ may operate in parallel to these cues by reinforcing those right-specific contacts that should persist, while insufficient adhesion on the left side contributes to selective elimination. In knockdown conditions, these stabilization signals are weakened and imbalanced, making left-side retention more likely.

An important future goal is identifying the Dpr-expressing partner population within the AB. Whether vΔ neurons themselves express one of the relevant Dprs, or whether an intermediate or postsynaptic third neuron provides the complementary adhesion surface, remains unknown. Combining single-cell transcriptomics, in situ labeling of Dpr genes, and cell-type-specific CRISPR knockouts will be essential for identifying these partners. Testing individual Dpr candidates (6, 13, 16, 19, 20) using targeted RNAi or CRISPR loss-of-function would directly evaluate whether DIP ζ's role in AB asymmetry depends on one specific ligand or multiple redundant partners.

Overall, the model emerging from this study is that DIP ζ acts as a membrane-anchored stabilizer of right-hemisphere connectivity. By forming selective DIP-Dpr adhesion complexes, it reinforces asymmetric wiring during the critical window of pupal remodeling. When DIP ζ is reduced, the stabilization mechanism becomes insufficient, and the system defaults toward symmetric or persistent left-side projections. This mechanism integrates intrinsic (cell-adhesion-based recognition) and extrinsic (midline and pruning cues) processes, offering a cohesive account of how developmental asymmetry in the Drosophila brain is achieved and maintained.

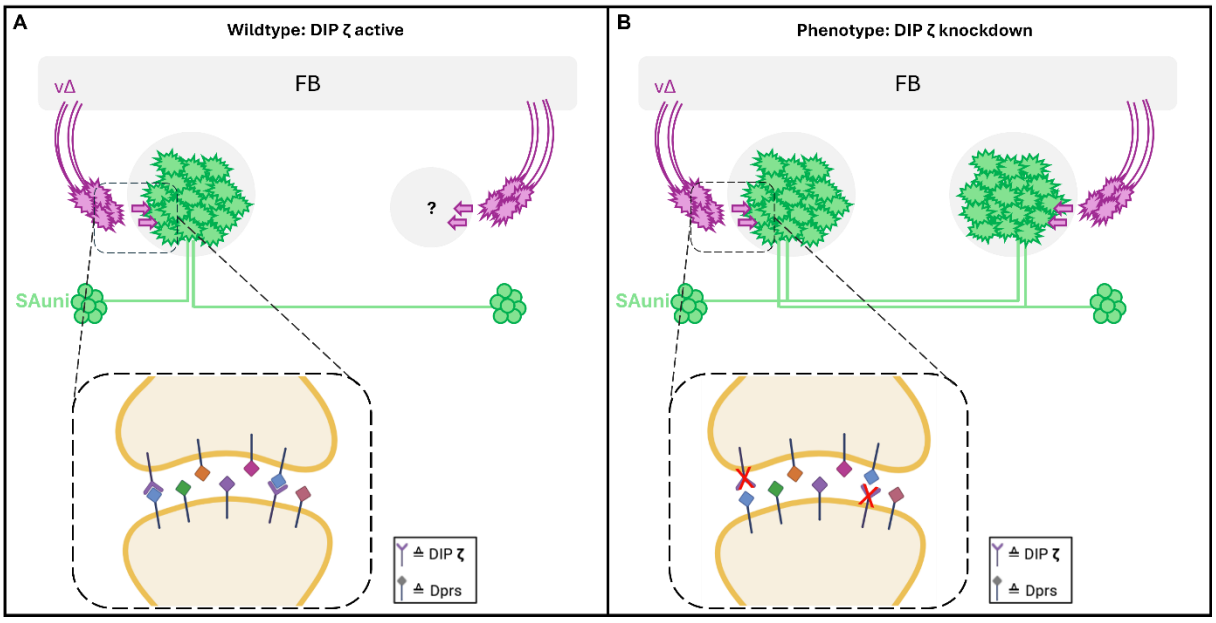

Figure 14. Proposed model of DIP ζ-dependent stabilization of asymmetric AB wiring:
This schematic summarizes a working model for how DIP ζ contributes to the establishment and maintenance of asymmetric AB connectivity during pupal development.

Wild-type condition (A):
In the intact system, DIP ζ is expressed on SA^{uni} neurons as well as on AB-associated target neurons, including vΔ neurons and potentially additional, as yet unidentified interneuron populations. At the right Asymmetrical Body (R-AB), DIP ζ engages one or more of its cognate Dpr partners, which are depicted as distinct Dpr molecules distributed along the neuronal membrane. These heterophilic DIP ζ-Dpr interactions promote selective adhesion at specific membrane contact sites, therby reinforcing right-sided synapses during pupal remodeling. In contrast, transient left-sided SA^{uni} projections lack sufficient matching Dpr partners or fail to reach the required adhesion strength and are therefore not stabilized, leading to their elimination during normal developmental pruning.

DIP ζ knockdown condition (B):
Upon RNAi-mediated reduction of DIP ζ in SA^{uni} and vΔ neurons, the membrane-anchored DIP ζ-Dpr adhesion interface cannot form. Although multiple Dpr proteins remain present on the neuronal membranes, the absence of DIP ζ prevents the formation of stabilizing heterophilic adhesion complexes. Consequently, right-sided synapses fail to be selectively stabilized. As a result, SA^{uni} projections do not maintain exclusive innervation of the R-AB, and left-sided contacts persist or re-emerge during late metamorphosis, giving rise to the observed bilateral AB innervation phenotype. Loss of preferential recognition by vΔ neurons is expected to further weaken circuit asymmetry.

Molecular close-up:
The lower panels depict a simplified representation of the proposed molecular organization at synaptic or pre-synaptic contact sites. Multiple Dpr isoforms are shown on the opposing membranes, reflecting the known binding repertoire of DIP ζ. Under wild-type conditions, DIP ζ molecules interact with one or several Dpr partners via their extracellular immunoglobulin-like domains, forming a selective adhesion interface. Following DIP ζ knockdown, Dpr proteins remain unbound and no stabilizing adhesion complex can be established. Because downstream intracellular signaling mechanisms of Dpr-DIP interactions remain poorly characterized, the model emphasizes their established role as membrane-tethered recognition and adhesion molecules rather than proposing specific intracellular signaling pathways. Together, this model provides a molecular framework explaining selective stabilization of right-sided AB connections in wild-type animals and the loss of asymmetry observed following DIP ζ depletion.

Abbreviations: AB = Asymmetrical Body; FB = fan-shaped body; DIP ζ = Dpr interacting protein ζ; Dpr = defective proboscis extension respronse; R-AB = right Asymmetrical Body.

5. Conclusion

This study employed a targeted RNAi screen to identify molecular regulators of structural brain asymmetry in *D. melanogaster*, focusing on the lateralized architecture of the Asymmetrical Body (AB). Among 20 tested candidates, Dpr-interacting protein ζ (DIP ζ) emerged as the only gene whose knockdown consistently increased bilateral AB innervation across multiple driver combinations. These results indicate that DIP ζ contributes to the molecular machinery required to restrict AB connectivity to the right hemisphere.

Developmental analysis further showed that bilateral phenotypes were already present during pupal metamorphosis when both SA^{uni} and vΔ neurons were targeted together, suggesting that DIP ζ acts during the remodeling phase in which transient bilateral projections are refined into a stable asymmetric pattern. The absence of a pupal phenotype, but presence of an adult phenotype, when SA^{uni} neurons were targeted alone implies that DIP ζ may operate across multiple developmental windows or cell types, and that full penetrance requires simultaneous disruption in both populations.

Taken together, the DIP ζ-Dpr interactions identified here, in conjunction with previous findings implicating Fas2 in stabilizing AB projections, highlight that the maintenance and remodeling of asymmetric circuits rely on a coordinated set of cell-adhesion molecules. Identifying DIP ζ as a part of this molecular repertoire emphasizes the contribution of IgSF-mediated adhesion codes to hemisphere-specific wiring. This work establishes a framework for future studies to map the relevant Dpr partners, dissect temporal requirements of DIP ζ function, and ultimately link structural asymmetry to behavioral outcomes such as memory and nagation.

6. Acknowledgements

First and foremost, I would like to express my sincere gratitude to Prof. Thomas Hummel for giving me the opportunity to conduct my master's thesis in his laboratory and for providing an inspiring research environment.

I am deeply thankful to Alexandra Grimm, Wolfgang Kallina, Daniela Bartel, and Sigrid Ilgerl for their continuous help and support whenever I faced technical or administrative challenges. Their assistance made it possible for me to focus fully on my research.

My heartfelt thanks go to the PhD students Daniel Mitić, Alisa Jiménez García, and Johann Markovitsch for their valuable guidance and supervision throughout my time in the lab and during the writing of this thesis. I am especially grateful to Aygül Bilge, who patiently explained many concepts to me when I first joined the lab and always offered her support whenever the workload became demanding.

Lastly, I would like to thank all members of the Hummel Lab for creating such a friendly, collaborative, and enjoyable working atmosphere. Their kindness and enthusiasm made my time in the lab a truly rewarding and memorable experience.

7. References

Anfora, G., Frasnelli, E., Maccagnani, B., Rogers, L. J., & Vallortigara, G. (2010). Behavioural and electrophysiological lateralization in a social (Apis mellifera) but not in a non-social (Osmia cornuta) species of bee. *Behavioural brain research*, *206*(2), 236-239. https://doi.org/10.1016/j.bbr.2009.09.023

Ashley, J., Sorrentino, V., Lobb-Rabe, M., Nagarkar-Jaiswal, S., Tan, L., Xu, S., Xiao, Q., Zinn, K., & Carrillo, R. A. (2019). Transsynaptic interactions between IgSF proteins DIP-α and Dpr10 are required for motor neuron targeting specificity. *eLife*, *8*, e42690. https://doi.org/10.7554/eLife.42690

Bisazza, A., Rogers, L. J., & Vallortigara, G. (1998). The origins of cerebral asymmetry: a review of evidence of behavioural and brain lateralization in fishes, reptiles and amphibians. *Neuroscience and biobehavioral reviews*, *22*(3), 411-426. https://doi.org/10.1016/s0149-7634(97)00050-x

Bleich-Cohen, M., Hendler, T., Kotler, M., & Strous, R. D. (2009). Reduced language lateralization in first-episode schizophrenia: an fMRI index of functional asymmetry. *Psychiatry research*, *171*(2), 82-93. https://doi.org/10.1016/j.pscychresns.2008.03.002

Bornstein, B., Meltzer, H., Adler, R., Alyagor, I., Berkun, V., Cummings, G., Reh, F., Keren-Shaul, H., David, E., Riemensperger, T., & Schuldiner, O. (2021). Transneuronal Dpr12/DIP-δ interactions facilitate compartmentalized dopaminergic innervation of Drosophila mushroom body axons. *The EMBO journal*, *40*(12), e105763. https://doi.org/10.15252/embj.2020105763

Brad K Hulse, Hannah Haberkern, Romain Franconville, Daniel Turner-Evans, Shin-ya Takemura, Tanya Wolff, Marcella Noorman, Marisa Dreher, Chuntao Dan, Ruchi Parekh, Ann M Hermundstad, Gerald M Rubin, Vivek Jayaraman (2021) A connectome of the Drosophila central complex reveals network motifs suitable for flexible navigation and context-dependent action selection eLife 10:e66039. https://doi.org/10.7554/eLife.66039

Brand, A. H., & Perrimon, N. (1993). Targeted gene expression as a means of altering cell fates and generating dominant phenotypes. *Development (Cambridge, England)*, *118*(2), 401-415. https://doi.org/10.1242/dev.118.2.401

Broca PP. Sur le siège de la Faculté du langage articulé. Bull Soc Anthropol Paris 6: 377-393, 1865.

Carrillo, R. A., Özkan, E., Menon, K. P., Nagarkar-Jaiswal, S., Lee, P. T., Jeon, M., Birnbaum, M. E., Bellen, H. J., Garcia, K. C., & Zinn, K. (2015). Control of Synaptic Connectivity by a Network of Drosophila IgSF Cell Surface Proteins. *Cell*, *163*(7), 1770-1782. https://doi.org/10.1016/j.cell.2015.11.022

Chen, C. C., Wu, J. K., Lin, H. W., Pai, T. P., Fu, T. F., Wu, C. L., Tully, T., & Chiang, A. S. (2012). Visualizing long-term memory formation in two neurons of the Drosophila brain. *Science (New York, N.Y.)*, *335*(6069), 678-685. https://doi.org/10.1126/science.1212735

Corballis, M. C. (2020). How many lateralities? *Laterality*, *26*(3), 307-309. https://doi.org/10.1080/1357650X.2020.1849251

Cosmanescu, F., Katsamba, P. S., Sergeeva, A. P., Ahlsen, G., Patel, S. D., Brewer, J. J., Tan, L., Xu, S., Xiao, Q., Nagarkar-Jaiswal, S., Nern, A., Bellen, H. J., Zipursky, S. L., Honig, B., & Shapiro, L. (2018). Neuron-Subtype-Specific Expression, Interaction Affinities, and Specificity Determinants of DIP/Dpr Cell Recognition Proteins. *Neuron*, *100*(6), 1385-1400.e6. https://doi.org/10.1016/j.neuron.2018.10.046

Couto, A., Alenius, M., & Dickson, B. J. (2005). Molecular, anatomical and functional organization of the Drosophila olfactory system. *Current biology : CB*, *15*(17), 1535-1547. https://doi.org/10.1016/j.cub.2005.07.034

Davis R. L. (2005). Olfactory memory formation in Drosophila: from molecular to systems neuroscience. *Annual review of neuroscience*, *28*, 275-302. https://doi.org/10.1146/annurev.neuro.28.061604.135651

Dietzl, G., Chen, D., Schnorrer, F., Su, K. C., Barinova, Y., Fellner, M., Gasser, B., Kinsey, K., Oppel, S., Scheiblauer, S., Couto, A., Marra, V., Keleman, K., & Dickson, B. J. (2007). A genome-wide transgenic RNAi library for conditional gene inactivation in Drosophila. *Nature*, *448*(7150), 151-156. https://doi.org/10.1038/nature05954

Duffy J. B. (2002). GAL4 system in Drosophila: a fly geneticist's Swiss army knife. *Genesis (New York, N.Y. : 2000)*, *34*(1-2), 1-15. https://doi.org/10.1002/gene.10150

Floris, D. L., Wolfers, T., Zabihi, M., Holz, N. E., Zwiers, M. P., Charman, T., Tillmann, J., Ecker, C., Dell'Acqua, F., Banaschewski, T., Moessnang, C., Baron-Cohen, S., Holt, R., Durston, S., Loth, E., Murphy, D. G. M., Marquand, A., Buitelaar, J. K., Beckmann, C. F., & EU-AIMS Longitudinal European Autism Project Group (2021). Atypical Brain Asymmetry in Autism-A Candidate for Clinically Meaningful Stratification. *Biological psychiatry. Cognitive neuroscience and neuroimaging*, *6*(8), 802-812. https://doi.org/10.1016/j.bpsc.2020.08.008

FlyBase. (accessed 2025). Dmel\DIP-ζ gene report. https://flybase.org/reports/FBgn0051708.html

Garbe, D. S., & Bashaw, G. J. (2007). Independent functions of Slit-Robo repulsion and Netrin-Frazzled attraction regulate axon crossing at the midline in Drosophila. *The Journal of neuroscience : the official journal of the Society for Neuroscience*, *27*(13), 3584-3592. https://doi.org/10.1523/JNEUROSCI.0301-07.2007

Graham J. H. (2022). Introduction to the special issue on symmetry in the life sciences-symmetry and asymmetry across biological scales. *Emerging topics in life sciences*, ETLS20210265. Advance online publication. https://doi.org/10.1042/ETLS20210265

Güntürkün, O., Ströckens, F., & Ocklenburg, S. (2020). Brain Lateralization: A Comparative Perspective. *Physiological reviews*, *100*(3), 1019-1063. https://doi.org/10.1152/physrev.00006.2019

Hanesch, U., Fischbach, K.F. & Heisenberg, M. Neuronal architecture of the central complex in *Drosophila melanogaster* . *Cell Tissue Res.* **257**, 343-366 (1989). https://doi.org/10.1007/BF00261838

Heinze, S., & Homberg, U. (2008). Neuroarchitecture of the central complex of the desert locust: Intrinsic and columnar neurons. *The Journal of comparative neurology*, *511*(4), 454-478. https://doi.org/10.1002/cne.21842

Hortsch M. (1996). The L1 family of neural cell adhesion molecules: old proteins performing new tricks. *Neuron*, *17*(4), 587-593. https://doi.org/10.1016/s0896-6273(00)80192-0

Jefferis, G. S., Potter, C. J., Chan, A. M., Marin, E. C., Rohlfing, T., Maurer, C. R., Jr, & Luo, L. (2007). Comprehensive maps of Drosophila higher olfactory centers: spatially segregated fruit and pheromone representation. *Cell*, *128*(6), 1187-1203. https://doi.org/10.1016/j.cell.2007.01.040

Jenett, A., Rubin, G. M., Ngo, T. T., Shepherd, D., Murphy, C., Dionne, H., Pfeiffer, B. D., Cavallaro, A., Hall, D., Jeter, J., Iyer, N., Fetter, D., Hausenfluck, J. H., Peng, H., Trautman, E. T., Svirskas, R. R., Myers, E. W., Iwinski, Z. R., Aso, Y., DePasquale, G. M., … Zugates, C. T. (2012). A GAL4-driver line resource for Drosophila neurobiology. *Cell reports*, *2*(4), 991-1001. https://doi.org/10.1016/j.celrep.2012.09.011

Kaiser M. (2017). Mechanisms of Connectome Development. *Trends in cognitive sciences*, *21*(9), 703-717. https://doi.org/10.1016/j.tics.2017.05.010

Kidd, T., Bland, K. S., & Goodman, C. S. (1999). Slit is the midline repellent for the robo receptor in Drosophila. *Cell*, *96*(6), 785-794. https://doi.org/10.1016/s0092-8674(00)80589-9

Kiral, F. R., Dutta, S. B., Linneweber, G. A., Hilgert, S., Poppa, C., Duch, C., von Kleist, M., Hassan, B. A., & Hiesinger, P. R. (2021). Brain connectivity inversely scales with developmental temperature in Drosophila. *Cell reports*, *37*(12), 110145. https://doi.org/10.1016/j.celrep.2021.110145

Lapraz, F., Boutres, C., Fixary-Schuster, C., De Queiroz, B. R., Plaçais, P. Y., Cerezo, D., Besse, F., Préat, T., & Noselli, S. (2023). Asymmetric activity of NetrinB controls laterality of the Drosophila brain. *Nature communications*, *14*(1), 1052. https://doi.org/10.1038/s41467-023-36644-4

Luan, H., Peabody, N. C., Vinson, C. R., & White, B. H. (2006). Refined spatial manipulation of neuronal function by combinatorial restriction of transgene expression. *Neuron*, *52*(3), 425-436. https://doi.org/10.1016/j.neuron.2006.08.028

Markovitsch J., Mitic D., Jiménez-Garcia A., Alsberga Z., Kainz S., Kaur R. & Hummel T. (2025). Sequential formation of Drosophila circuit asymmetry via prolonged structural plasticity. https://doi.org/10.1101/2025.05.27.656373

Mitic D., unpublished Master Thesis (2021)

Mitic et al., manuscript in prep. (2025)

Morano, N. C., Lopez, D. H., Meltzer, H., Sergeeva, A. P., Katsamba, P. S., Rostam, K. D., Gupta, H. P., Becker, J. E., Bornstein, B., Cosmanescu, F., Schuldiner, O., Honig, B., Mann, R. S., & Shapiro, L. (2025). Members of the DIP and Dpr adhesion protein families use cis inhibition to shape neural development in Drosophila. *PLoS biology*, *23*(3), e3003030. https://doi.org/10.1371/journal.pbio.3003030

National Institutes of Health (NIH). (2024). Researchers fully map neural connections of the adult fruit fly brain. *NIH Research Matters*. Retrieved from https://www.nih.gov/news-events/nih-research-matters/complete-wiring-map-adult-fruit-fly-brain

Nielsen, J.A., Zielinski, B.A., Fletcher, P.T. *et al.* Abnormal lateralization of functional connectivity between language and default mode regions in autism. *Molecular Autism* **5**, 8 (2014). https://doi.org/10.1186/2040-2392-5-8

Özkan, E., Carrillo, R. A., Eastman, C. L., Weiszmann, R., Waghray, D., Johnson, K. G., Zinn, K., Celniker, S. E., & Garcia, K. C. (2013). An extracellular interactome of immunoglobulin and LRR proteins reveals receptor-ligand networks. *Cell*, *154*(1), 228-239. https://doi.org/10.1016/j.cell.2013.06.006

Pascual, A., Huang, KL., Neveu, J. *et al.* Brain asymmetry and long-term memory. *Nature* 427, 605-606 (2004). https://doi.org/10.1038/427605a

Peng, I. F., Berke, B. A., Zhu, Y., Lee, W. H., Chen, W., & Wu, C. F. (2007). Temperature-dependent developmental plasticity of Drosophila neurons: cell-autonomous roles of membrane excitability, Ca2+ influx, and cAMP signaling. *The Journal of neuroscience : the official journal of the Society for Neuroscience*, *27*(46), 12611-12622. https://doi.org/10.1523/JNEUROSCI.2179-07.2007

Perkins, L. A., Holderbaum, L., Tao, R., Hu, Y., Sopko, R., McCall, K., Yang-Zhou, D., Flockhart, I., Binari, R., Shim, H. S., Miller, A., Housden, A., Foos, M., Randkelv, S., Kelley, C., Namgyal, P., Villalta, C., Liu, L. P., Jiang, X., Huan-Huan, Q., … Perrimon, N. (2015). The Transgenic RNAi Project at Harvard Medical School: Resources and Validation. *Genetics*, *201*(3), 843-852. https://doi.org/10.1534/genetics.115.180208

Pfeiffer, B. D., Ngo, T. T., Hibbard, K. L., Murphy, C., Jenett, A., Truman, J. W., & Rubin, G. M. (2010). Refinement of tools for targeted gene expression in Drosophila. *Genetics*, *186*(2), 735-755. https://doi.org/10.1534/genetics.110.119917

Pfeiffer, K., & Homberg, U. (2014). Organization and functional roles of the central complex in the insect brain. *Annual review of entomology*, *59*, 165-184. https://doi.org/10.1146/annurev-ento-011613-162031

Port, F., Strein, C., Stricker, M., Rauscher, B., Heigwer, F., Zhou, J., Beyersdörffer, C., Frei, J., Hess, A., Kern, K., Lange, L., Langner, N., Malamud, R., Pavlović, B., Rädecke, K., Schmitt, L., Voos, L., Valentini, E., & Boutros, M. (2020). A large-scale resource for tissue-specific CRISPR mutagenesis in *Drosophila*. *eLife*, *9*, e53865. https://doi.org/10.7554/eLife.53865

Postema, M.C., van Rooij, D., Anagnostou, E. *et al.* Altered structural brain asymmetry in autism spectrum disorder in a study of 54 datasets. *Nat Commun* **10**, 4958 (2019). https://doi.org/10.1038/s41467-019-13005-8

Riebli, N., Viktorin, G., & Reichert, H. (2013). Early-born neurons in type II neuroblast lineages establish a larval primordium and integrate into adult circuitry during central complex development in Drosophila. *Neural development*, *8*, 6. https://doi.org/10.1186/1749-8104-8-6

Rogers, L. J. (1995). Evolution and development of brain asymmetry and its relevance to language, tool and consciousness. *Int. J. Comparative Psychology*, 8(1), 5-23. https://doi.org/10.46867/C48594

Rogers, L. J., Vallortigara, G., & Andrew, R. J. (2013). *Divided brains: The biology and behaviour of brain asymmetries.* Cambridge University Press. https://doi.org/10.1017/CBO9780511793899

Sakamura, S., Hsu, F. Y., Tsujita, A., Abubaker, M. B., Chiang, A. S., & Matsuno, K. (2023). Ecdysone signaling determines lateral polarity and remodels neurites to form Drosophila's left-right brain asymmetry. *Cell reports*, *42*(4), 112337. https://doi.org/10.1016/j.celrep.2023.112337

Sanders, L. (2024, October 2). Scientists trace every neuron and connection in a fruit fly brain. *Science News*. Retrieved from https://www.sciencenews.org/article/fruit-fly-brain-connections-traced

Scheffer, L. K., Xu, C. S., Januszewski, M., Lu, Z., Takemura, S. Y., Hayworth, K. J., Huang, G. B., Shinomiya, K., Maitlin-Shepard, J., Berg, S., Clements, J., Hubbard, P. M., Katz, W. T., Umayam, L., Zhao, T., Ackerman, D., Blakely, T., Bogovic, J., Dolafi, T., Kainmueller, D., … Plaza, S. M. (2020). *A connectome and analysis of the adult Drosophila central brain.* eLife, 9, e57443. https://doi.org/10.7554/eLife.57443

Schindelin, J., Arganda-Carreras, I., Frise, E., Kaynig, V., Longair, M., Pietzsch, T., Preibisch, S., Rueden, C., Saalfeld, S., Schmid, B., Tinevez, J. Y., White, D. J., Hartenstein, V., Eliceiri, K., Tomancak, P., & Cardona, A. (2012). Fiji: an open-source platform for biological-image analysis. *Nature methods*, *9*(7), 676-682. https://doi.org/10.1038/nmeth.2019

Schlegel, P., Yin, Y., Bates, A. S., Dorkenwald, S., Eichler, K., Brooks, P., Han, D. S., Gkantia, M., Dos Santos, M., Munnelly, E. J., Badalamente, G., Serratosa Capdevila, L., Sane, V. A., Fragniere, A. M. C., Kiassat, L., Pleijzier, M. W., Stürner, T., Tamimi, I. F. M., Dunne, C. R., Salgarella, I., … Jefferis, G. S. X. E. (2024). Whole-brain annotation and multi-connectome cell typing of Drosophila. *Nature*, *634*(8032), 139-152. https://doi.org/10.1038/s41586-024-07686-5

Sergeeva, A. P., Katsamba, P. S., Cosmanescu, F., Brewer, J. J., Ahlsen, G., Mannepalli, S., Shapiro, L., & Honig, B. (2020). DIP/Dpr interactions and the evolutionary design of specificity in protein families. *Nature communications*, *11*(1), 2125. https://doi.org/10.1038/s41467-020-15981-8

Sha, Z., Schijven, D., Carrion-Castillo, A. *et al.* The genetic architecture of structural left-right asymmetry of the human brain. *Nat Hum Behav* 5, 1226-1239 (2021). https://doi.org/10.1038/s41562-021-01069-w

Sha, Z., Schijven, D., & Francks, C. (2021). Patterns of brain asymmetry associated with polygenic risks for autism and schizophrenia implicate language and executive functions but not brain masculinization. *Molecular psychiatry*, *26*(12), 7652-7660. https://doi.org/10.1038/s41380-021-01204-z

Strausfeld, N. J. (2012). *Arthropod Brains: Evolution, Functional Elegance, and Historical Significance*. Harvard University Press. https://doi.org/10.2307/j.ctv1dp0v2h

Strauss R. (2002). The central complex and the genetic dissection of locomotor behaviour. *Current opinion in neurobiology*, *12*(6), 633-638. https://doi.org/10.1016/s0959-4388(02)00385-9

Tan, L., Zhang, K. X., Pecot, M. Y., Nagarkar-Jaiswal, S., Lee, P. T., Takemura, S. Y., McEwen, J. M., Nern, A., Xu, S., Tadros, W., Chen, Z., Zinn, K., Bellen, H. J., Morey, M., & Zipursky, S. L. (2015). Ig Superfamily Ligand and Receptor Pairs Expressed in Synaptic Partners in Drosophila. *Cell*, *163*(7), 1756-1769. https://doi.org/10.1016/j.cell.2015.11.021

Ting, C. Y., Gu, S., Guttikonda, S., Lin, T. Y., White, B. H., & Lee, C. H. (2011, May). Focusing transgene expression in drosophila by Coupling GAL4 with a Novel Split-Lex A Expression System. *Genetics*. https://doi.org/10.1534/genetics.110.126193

Toga, A. W., Narr, K. L., Thompson, P. M., & Luders, E. (2009). Brain asymmetry: Evolution. In *Encyclopedia of Neuroscience* (pp. 303-311). Elsevier Ltd.. https://doi.org/10.1016/B978-008045046-9.00936-0

Truman, J. W., & Riddiford, L. M. (2023). Drosophila postembryonic nervous system development: a model for the endocrine control of development. *Genetics*, *223*(3), iyac184. https://doi.org/10.1093/genetics/iyac184

Veverytsa, L., & Allan, D. W. (2013). Subtype-specific neuronal remodeling during Drosophila metamorphosis. *Fly*, *7*(2), 78-86. https://doi.org/10.4161/fly.23969

Wolff, T., & Rubin, G. M. (2018). Neuroarchitecture of the Drosophila central complex: A catalog of nodulus and Asymmetrical Body neurons and a revision of the protocerebral bridge catalog. *The Journal of comparative neurology*, *526*(16), 2585-2611. https://doi.org/10.1002/cne.24512

Wu, J. S., & Luo, L. (2006). A protocol for dissecting Drosophila melanogaster brains for live imaging or immunostaining. *Nature protocols*, *1*(4), 2110-2115. https://doi.org/10.1038/nprot.2006.336

Yu, F., & Schuldiner, O. (2014). Axon and dendrite pruning in Drosophila. *Current opinion in neurobiology*, *27*, 192-198. https://doi.org/10.1016/j.conb.2014.04.005